
The Value of Mechanistic Priors in Sequential Decision Making

Itai Shufaro*
Technion

Gal Benor*
Technion

Shie Mannor
Technion, NVIDIA Research

Abstract

Hybrid mechanistic models, physical priors with learned residuals, promise to reduce the data required for good decisions, but have no computable criterion to test this. We characterize the value of mechanistic priors in sequential decision-making within both asymptotic and burn-in regimes. To formalize this, we introduce the *mechanistic information* of a model—the mutual information between the model’s recommended policy $\hat{\pi}$ and the true optimal policy π^* —quantified via an occupancy-weighted bias B_μ . In the *asymptotic regime* (large N), matched bounds reveal that Bayesian regret scales with the residual entropy H_{mech} , delivering a theoretical sample complexity reduction of $H(\mu)/H_{\text{mech}}$ compared to an uninformed baseline. Furthermore, we provide a model certificate to determine empirical sample efficiency. Complementarily, in the clinically relevant *burn-in regime* (small N), we establish a lower bound on the penalty incurred by confidently wrong priors. We demonstrate both the asymptotic and burn-in bounds across 5-fluorouracil (5-FU) dosing simulations motivated by published FOLFOX pharmacokinetic data, where a hybrid prior yields large sample-efficiency gains in the burn-in regime. Finally, we contrast these grounded models with LLM priors, demonstrating that LLMs can suffer severe losses in mechanistic information, thereby motivating the exclusive use of physically-grounded priors for safety-critical applications.

1 Introduction

Hybrid mechanistic models—known dynamics paired with learned residuals—are pervasive in scientific machine learning and increasingly central to adaptive medicine: universal differential equations [30], physics-informed neural networks [21], grey-box pharmacokinetic models, and the digital twins underlying in silico clinical trials [10] all share the same structural premise. The premise is that physical structure reduces the data required to reach good decisions, and it is taken for granted in practice. Yet there is no computable, pre-trial criterion that tells a decision-maker whether a specific hybrid model will save samples on a specific sequential task. This is the goal of this paper.

Information-theoretic bounds connecting prior information to sample complexity already exist for other online settings. Russo and Van Roy [33] show that the Bayesian regret of Thompson sampling on a K -armed bandit scales with the entropy of the optimal arm, and Shufaro et al. [37] extend this to a regret–information trade-off that quantifies the value of R nats of side information. Both lines treat the prior as exogenous: R nats arrive from somewhere and are used. We focus on extending their contribution by calculating the value of mechanistic models.

*Equal contribution. Correspondence to: itai.shufaro@campus.technion.ac.il, gal.benor@campus.technion.ac.il

1.1 Contributions

Mechanistic information and critical bias We define *mechanistic information* $R_{\text{mech}} = I(\pi^*; \hat{\pi})$, the mutual information between the model’s recommended policy $\hat{\pi}$ and the optimal policy π^* , and bound it through an occupancy-weighted bias B_μ that charges the model only for errors the optimal policy actually visits. From this bound, we derive the *critical bias* B_μ^{crit} : a closed-form quantity computable from calibration data alone that certifies, before any interaction is made, whether a candidate model will reduce sample complexity at horizon N .

Matched regret bounds Extending the framework of Shufaro et al. [37] to mechanistic models, we prove matching upper and lower bounds on Bayesian regret, tight up to a $\sqrt{\log K}$ factor. The bounds scale with the *residual entropy* $H_{\text{mech}} = H(\mu) - R_{\text{mech}}$, yielding a sample-complexity reduction of $H(\mu)/H_{\text{mech}}$ relative to an uninformed baseline. This tightness is what makes the certificate quantitative: it pins B_μ^{crit} to a specific operational target rather than an order-of-magnitude estimate.

Burn-in regime We derive a lower bound on the regret suffered when the prior is concentrated but potentially wrong. This setting is especially relevant when using a population-calibrated model for an individual patient, making this bound applicable for a medical setting. We also demonstrate that LLM priors can significantly degrade performance, motivating the use of physically-grounded priors in safety-critical settings.

Paper organization. Section 2 formalizes the reduction to a bandit reduction and introduces mechanistic information. Section 3 proves the asymptotic results and presents the model-quality certificate. Section 4 proves the burn-in and LLM results. Section 5 presents the clinical instantiation and simulation. Sections 6 and 7 place the work in context.

2 Setting

This section formalizes the reduction from the continuous control problem to a K -armed policy bandit and introduces the central quantity R_{mech} . This frames our problem as policy selection, which is equivalent to selecting an entire treatment strategy upfront rather than selecting individual doses.

2.1 Reduction to policy bandit

The mechanistic model \mathcal{M} defines a distribution over the dynamics of the continuous control problem: Given a control signal $u(t)$ and a state trajectory $x(t)$, the cumulative reward is $J(u; \mathcal{M}) = \int_0^T \ell(x(t), u(t)) dt$. The *true optimal policy* is $\pi^* = \arg \max_{u \in \mathcal{U}} J(u; \mathcal{M}^*)$, where \mathcal{M}^* is the unknown true dynamics. We discretize the control space into K representative policies, $\Pi = \{\pi_1, \dots, \pi_K\}$ (e.g. via a finite-difference grid on the infusion rate), reducing our control problem to a K-MAB one. Each policy π_k has mean reward $\bar{r}(\pi_k) = J(\pi_k; \mathcal{M}^*)$. At round t the learner plays $\pi_t \in \Pi$ and observes $r_t = \bar{r}(\pi_t) + \xi_t$, where ξ_t is zero-mean with standard deviation $\sigma_\xi > 0$. We make the following assumption regarding the rewards of the policy class.

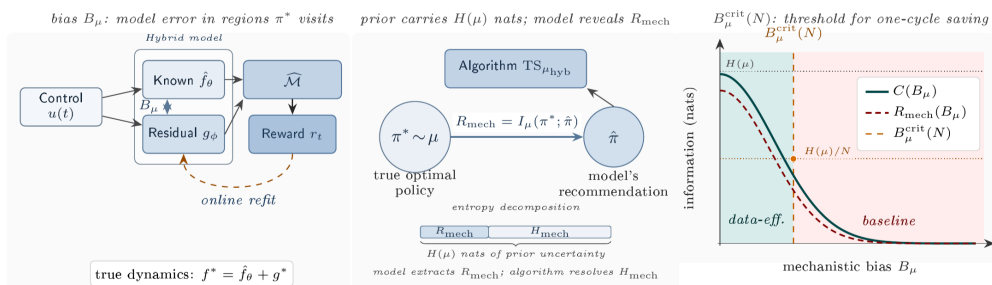


Figure 1: Three layers of the hybrid model learning setting. (A) Mechanistic model. (B) Information flow from π^* to $\hat{\pi}$ and to the environment. (C) Regret-bias diagram: switching regimes at B_μ^{crit} .

Assumption 1 (Discretization quality) *The policy π^* belongs to Π , or the best policy in Π has sub-optimality gap at most $\Delta_r/2$ relative to the continuous optimum,*

$$J(\pi^*; \mathcal{M}^*) - \max_{\pi \in \Pi} J(\pi; \mathcal{M}^*) \leq \frac{\Delta_r}{2}. \quad (1)$$

The mechanistic model \mathcal{M} recommends the best policy in Π under the approximate dynamics,

$$\hat{\pi} = \arg \max_{\pi \in \Pi} J(\pi; \hat{\mathcal{M}}). \quad (2)$$

This policy is computable from the model $\hat{\mathcal{M}}$ alone, without knowing the true dynamics. We remark that $\hat{\pi}$ is not the policy for which the model is most accurate everywhere, but rather it is the policy that performs best under the model’s predictions. Even an inaccurate model can produce a useful $\hat{\pi}$ if its prediction errors cancel in the reward integral. The optimal policy π^* is drawn from a prior μ on Π (reflecting our uncertainty about \mathcal{M}^* before any interaction). We write $H(\mu)$ for the Shannon entropy of the prior μ over Π . All logarithms are natural (nats) unless explicitly labeled \log_2 (bits). We use the Bayesian regret, which is the mean gap between the optimal and chosen rewards over the randomness present in the prior, π^* , and the algorithm. This metric measures the prior’s worth in terms of interactions saved.

Definition 1 (Bayesian regret)

$$\text{BR}^*(N) = \mathbb{E}_{\pi^* \sim \mu} \mathbb{E} \left[\sum_{t=1}^N (\bar{r}(\pi^*) - \bar{r}(\pi_t)) \right].$$

2.2 Occupancy-weighted sensitivity

Assumption 2 (Metric model space) *The model space is metric, with norm $\|\mathcal{M} - \mathcal{M}'\|$.*

Assumption 3 (Occupancy-weighted Lipschitz sensitivity) *There exists $\kappa_\mu > 0$ such that for any two models, $\mathcal{M}, \mathcal{M}'$ and $B > 0$ such that $\|\mathcal{M} - \mathcal{M}'\| \leq B$,*

$$\|\pi^*(\mathcal{M}) - \pi^*(\mathcal{M}')\|_{\Pi} \leq \kappa_\mu B,$$

where $\|\cdot\|_{\Pi}$ is any metric on the discrete policy class (e.g. 0–1 distance).

The occupancy weighting charges the model only for errors in regions π^* actually visits. Concretely,

$$B_\mu = \sqrt{\sum_{k=1}^K \mu(\pi_k) (J(\pi_k; \mathcal{M}^*) - J(\pi_k; \hat{\mathcal{M}}))^2} \quad (3)$$

is the prior-weighted RMS reward gap between true and modeled dynamics. A model that is inaccurate in corners of the state space that the optimal policy never reaches has a small B_μ and transfers many bits. A model that is slightly wrong exactly where the optimum operates has a large B_μ and transfers almost none. While Assumption 3 appears restrictive at first, it is achieved under standard regularity conditions for ODE models (which are common in medical settings, see Lemma 1 in Appendix D).

Assumption 4 *The residual reward $g^* = J(u_t; \mathcal{M}^*) - J(u_t; \hat{\mathcal{M}})$ is drawn from a Gaussian process with marginal variance $\sigma_{\mathcal{F}}^2$ per dimension and effective dimension $d_{\mathcal{F}}$ (rank of the kernel operator of the GP, see Appendix H for more details).*

Using Assumption 4, we can tie the variance of the residual dynamics ($\sigma_{\mathcal{F}}^2$) and the prior’s entropy ($H(\mu)$). A richer prior (large $H(\mu)$) implies larger expected residuals (conservative), while a higher-dimensional residual class (large $d_{\mathcal{F}}$) implies smaller $\sigma_{\mathcal{F}}^2$ per dimension, since the same total uncertainty is spread across more dimensions. Throughout this paper, we use a running example, for illustration, based on adaptive dosing of 5-fluorouracil (5-FU) in colorectal cancer patients receiving FOLFOX.

Running Example 1 (Adaptive 5-FU dosing) The mechanistic model $\hat{\mathcal{M}}$ is a 3-compartment ODE tracking plasma 5-FU, intracellular FdUMP, free and inhibited thymidylate synthase, and a toxicity proxy. The policy class $\Pi = \{\pi_1, \dots, \pi_8\}$ ($K = 8$) represents eight dose levels spanning 1,600–3,600 mg/m², the clinical adjustment range in the Kaldate et al. [20] dataset. Reward $r_t \in \{0, 1\}$ indicates whether the 46-hour AUC falls within the therapeutic window 20–30 mg·h/L.

2.3 Mechanistic Information

Definition 2 (Mechanistic information)

$$R_{\text{mech}} = I_{\mu}(\pi^*; \hat{\pi}),$$

the mutual information between $\pi^* \sim \mu$ and the mechanistic recommendation $\hat{\pi}$ defined by (2).

R_{mech} measures the number of nats about π^* that the model reveals before a single interaction is performed. When $B_{\mu} = 0$, the model is exact, so $\hat{\pi} = \pi^*$ and $R_{\text{mech}} = H(\mu)$ (the model resolves all uncertainty). When $B_{\mu} \rightarrow \infty$, the model's error is so large that $\hat{\pi}$ is essentially independent of π^* , so $R_{\text{mech}} \rightarrow 0$ (the model contributes nothing). The residual entropy $H_{\text{mech}} = H(\mu) - R_{\text{mech}}$ quantifies the information the algorithm must discover by interacting with the system. We now introduce upper bounds for the mechanistic information and the residual entropy.

Proposition 1 (Mechanistic information bounds) *Under Assumptions 2–4:*

$$R_{\text{mech}}(B_{\mu}, \mathcal{F}) \leq C(B_{\mu}) := \frac{d_{\mathcal{F}}}{2} \log \left(1 + \frac{\kappa_{\mu}^2 \sigma_{\mathcal{F}}^2}{\kappa_{\mu}^2 B_{\mu}^2 + \sigma^2} \right). \quad (4)$$

Remark 1 *The upper bound $C(B_{\mu})$ is strictly decreasing in B_{μ} , from $C(0) = \frac{d_{\mathcal{F}}}{2} \log(1 + \kappa_{\mu}^2 \sigma_{\mathcal{F}}^2 / \sigma^2)$ to $C(\infty) = 0$. Under the canonical parametrization, $C(0) = \frac{d_{\mathcal{F}}}{2} \log(1 + 2H(\mu)/d_{\mathcal{F}}) \leq H(\mu)$ (with near-equality when $d_{\mathcal{F}} \gg H(\mu)$, since $\log(1+x) \approx x$ for small x). The bound is not vacuous at $B_{\mu} = 0$ when $\sigma > 0$: the reward noise places a floor on the channel capacity even for a perfect model.*

The proof is provided in Appendix D. The mechanistic model essentially acts as a noisy Gaussian channel—the model bias contributes noise variance $\kappa_{\mu}^2 B_{\mu}^2$, and reward observation noise contributes additional variance of σ^2 . Since both are independent, the total channel noise is $\kappa_{\mu}^2 B_{\mu}^2 + \sigma^2$, so the SNR decreases as B_{μ} grows. Bound (4) is an upper limit on how much information the model can transmit under model bias and noise constraints.

Running Example 2 (Mechanistic information for 5-FU) Using calibrated parameters ($K = 8$, $B_{\mu} = 0.22$, $\sigma = 0.40$, $\kappa_{\mu} = 1.8$, $d_{\mathcal{F}} = 3$. See Appendix H for the derivation). Prior entropy: $H(\mu) = \ln 8 \approx 2.08$ nats (uniform prior). The canonical GP std is $\sigma_{\mathcal{F}}^2 = 2\sigma^2 H(\mu)/(\kappa_{\mu}^2 d_{\mathcal{F}}) \approx 0.0685$, $\sigma_{\mathcal{F}} \approx 0.26$. We use this to calculate the capacity:

$$C(0.22) = \frac{3}{2} \ln \left(1 + \frac{1.8^2 \times 0.0685}{1.8^2 \times 0.22^2 + 0.40^2} \right) = \frac{3}{2} \ln(1.700) \approx 0.80 \text{ nats.}$$

The theory certifies $R_{\text{mech}} \leq 0.80$ nats. Since $C(0.22) \leq H(\mu)$, the bound is not vacuous here. Under the bound, $H_{\text{mech}} \geq H(\mu) - C(0.22) = 2.08 - 0.80 = 1.28$ nats.

3 Asymptotic Regime

3.1 Lower and Upper bounds

To quantify the regret's dependence on mechanistic information, we lower-bound the Bayesian regret using the residual entropy H_{mech} , and prove a matching upper bound up to a $\sqrt{\log K}$ factor.

Theorem 1 (Hybrid regret lower bound) *Consider the hybrid setting with K policies, N rounds, mechanistic bias B_{μ} , and prior μ on Π . Under Assumptions 2–4, for any algorithm, there exist universal constants $c, N_0 > 0$ such that for all $N \geq N_0$:*

$$\text{BR}^*(N) \geq c \sqrt{\frac{KN H_{\text{mech}}}{\log K}}, \quad (5)$$

where $H_{\text{mech}} = \max(H(\mu) - R_{\text{mech}}(B_{\mu}, \mathcal{F}), 0)$.

Theorem 1 quantifies how much regret can be avoided by utilizing the model. We have shown that R_{mech} quantifies how many nats of prior information the model “spends” before interaction starts. This reduces the effective problem from one with $H(\mu)$ to one with only H_{mech} nats of uncertainty. The lower bound certifies that no algorithm — even one that uses the prior optimally — can achieve regret better than $c\sqrt{KNH_{\text{mech}}/\log K}$. Thus, the ratio $\sqrt{H(\mu)/H_{\text{mech}}}$ quantifies the reduction in the regret that is obtained by following the model’s recommendation. The proof of Theorem 1 follows directly from Proposition 4.1 of Shufaro et al. [37], and is provided in Appendix E.

Theorem 2 (Thompson Sampling upper bound) *Assume $\mu = \text{Uniform}(\Pi)$. Let μ_{hyb} be the posterior of μ after conditioning on $\hat{\pi}$. By construction $I(\pi^*; \hat{\pi}) = R_{\text{mech}}$. Let TS_{hyb} be Thompson Sampling with this prior. Then there exists a universal constant $C > 0$ such that:*

$$\text{BR}_{\text{TS}_{\text{hyb}}}(N) \leq C\sqrt{KNH_{\text{mech}}}, \quad (6)$$

Theorem 2 shows that when the prior is concentrated on $\hat{\pi}$, Thompson Sampling with μ_{hyb} achieves the lower bound. When the prior is concentrated on $\hat{\pi}$, the algorithm’s first prediction identifies $\hat{\pi}$ with probability $\mu_{\text{hyb}}(\hat{\pi})$ (close to 1 when $R_{\text{mech}} \approx \log K$), and subsequent rounds refine or overturn this guess. The proof of Theorem 2 follows from [33] and can be found in Appendix E.

The upper and lower bounds also measure how many samples can be saved by utilizing the model’s prior. The sample complexity of a bandit algorithm is the number of rounds N needed to achieve mean regret smaller than ε . Combining Equations (5) and (6) in the asymptotic regime we obtain the asymptotic sample-complexity ratio:

$$\rho = \frac{N_{\text{uninf}}}{N_{\text{mech}}} = \Theta\left(\frac{H(\mu)}{H_{\text{mech}}}\right). \quad (7)$$

where the Θ notation omits factors of $\Theta(\log K)$.

Running Example 3 (Lower and upper bounds for 5-FU) We apply Theorems 1 and 2 to our conservative running example. With $K = 8$, $H_{\text{mech}} = 1.28$ nats (the bound certified in Example 2) and $N = 12$ cycles we get $7.7c \leq \text{BR}^*(12) \leq 11.1C$. The ratio $11.1/7.7 = 1.44 \approx \sqrt{\ln 8}$ is exactly the $\sqrt{\log K}$ slack between the two bounds. The sample-complexity ratio (Eq. (7)) is $\rho = H(\mu)/H_{\text{mech}} \approx 1.6$: even in the worst-case bound, TS without the hybrid prior needs $1.6\times$ more samples (cycles with wrong dosing) to reach the same regret. *Note:* a more informative mechanistic model – e.g. $R_{\text{mech}} = 1.9$, yields a much larger ratio of $\rho \approx 11.5\times$

3.2 Critical Bias

The previous section demonstrated how one can use information to effectively quantify regret improvement. However, to be more relevant in clinical settings, we need a quantity that is both relevant to the number of trials we realistically reduce, while also being computable without requiring any additional trials. This is the goal of this section.

We note that we can freely select rewards up to scaling. Thus, we adapt the following scaling, based on normalizing the variance of the residual reward, which we call the canonical parameterization.

Remark 2 (Canonical parametrization) *For the model-quality certificate (Theorem 3), we adopt the canonical parametrization $\sigma_{\mathcal{F}}^2 = 2\sigma^2 H(\mu)/(\kappa_{\mu}^2 d_{\mathcal{F}})$, chosen so that $C(0) \approx H(\mu)$ for $H(\mu) \ll d_{\mathcal{F}}$. ($C(0) = \frac{d_{\mathcal{F}}}{2} \log(1 + 2H(\mu)/d_{\mathcal{F}}) \leq H(\mu)$ exactly, with near-equality when $d_{\mathcal{F}} \gg H(\mu)$). All other results hold for arbitrary $\sigma_{\mathcal{F}}^2 > 0$.*

We now introduce the critical bias, which is a computable model certificate that governs the ability of the model to reduce sample complexity.

Theorem 3 (Critical bias) *Assume $R_{\text{mech}} > 0$. Under the canonical parametrization of Remark 2, define*

$$B_{\mu}^{\text{crit}}(N) = \frac{\sigma}{\kappa_{\mu}} \sqrt{\frac{2H(\mu)/d_{\mathcal{F}}}{e^{2H(\mu)/(d_{\mathcal{F}}N)} - 1}} - 1. \quad (8)$$

The following then holds:

- i* Data-efficient regime ($B_\mu < B_\mu^{\text{crit}}$): The model can reduce sample complexity by one or more cycles.
- ii* Baseline regime ($B_\mu \geq B_\mu^{\text{crit}}$): The model cannot reduce the sample complexity.

Theorem 3 defines the *critical bias* B_μ^{crit} as the bias at which the model’s information contribution matches a chosen operational target (e.g., saving one cycle, or one nat of information etc.). Below it, the model meaningfully constrains π^* . Above it, the recommendation is barely better than a random guess. The ratio $B_\mu/B_\mu^{\text{crit}}$ is a *model-quality certificate* computable from calibration data before any trial. The proof of Theorem 3 is provided in Appendix E.

Remark 3 *The critical bias can be defined relative to any operational working point: the formula (8) sets $C(B_\mu^{\text{crit}}) = H(\mu)/N$, i.e. the bias at which the model captures a $1/N$ fraction of the prior entropy and saves at least one cycle. Other working points (e.g. $N/2$ sample reduction, the one-nat boundary $C(B_\mu^{\text{crit}}) = 1$) yield analogous results, and may be more appropriate when the trial designer has a specific accuracy or sample-budget target.*

Running Example 4 (Model-quality certificate for 5-FU) Using existing datasets [20, 27] we get $\sigma = 0.40$, $\kappa_\mu = 1.8$, $H(\mu) = \ln 8 \approx 2.08$. We also fix $K = 8$ and $N = 12$. The critical bias $B_\mu^{\text{crit}} = 0.71$ (normalized units). Calibrated ODE: $B_\mu = 0.22 < B_\mu^{\text{crit}}$, well below the critical bias threshold. This indicates the calibrated ODE can provide at least one cycle reduction.

4 Finite-Sample Regime

4.1 Burn-in bound for misspecified priors

Section 3 characterized regret in the asymptotic regime. We now turn to the finite-sample regime relevant to clinical-trial design.

Proposition 2 (Burn-in lower bound) *Let the prior μ place probability $1 - \epsilon$ on $\hat{\pi}$ (confident but wrong) and ϵ on π^* , with sub-optimality gap $\Delta_r > 0$. Let $\delta \in (0, \frac{1}{2})$ and assume $\epsilon \leq \delta$. Any algorithm that identifies π^* with probability $\geq 1 - \delta$ suffers expected regret of at least*

$$\frac{(1 - \delta)(1 - \epsilon) \Delta_r \log[(1 - \epsilon)/\delta]}{\text{kl}(\epsilon_K, 1 - \epsilon_K)} \tag{9}$$

before identification, where $\text{kl}(p, q) = p \log(p/q) + (1 - p) \log((1 - p)/(1 - q))$ is the binary KL divergence, and $\epsilon_K = \epsilon/(1 - \epsilon + \epsilon K)$ is the effective prior weight on π^ across all K arms.*

Proposition 2 quantifies the minimum exploration cost that a confidently wrong prior forces. In particular, it is proportional to $\log[(1 - \epsilon)/\delta]$. Thus, an algorithm that uses a confidently wrong prior must accumulate significantly more nats of evidence to overcome the prior’s initial confidence in the wrong arm, significantly increasing its sample complexity. The cost grows logarithmically as the prior becomes more confident ($\epsilon \rightarrow 0$) or as the identification confidence requirement tightens ($\delta \rightarrow 0$). The proof of Proposition 2 follows from the Wald-Wolfowitz optimality of the SPRT [41] and can be found in Appendix F. Since the Wald-Wolfowitz bound is tight, the bound is not pessimistic.

Running Example 5 (Burn-in for a miscalibrated 5-FU prior) Using the $K = 8$ calibrated setting. Prior: $1 - \epsilon = 0.8$ on $\hat{\pi}$ (mechanistic model is confident but may be wrong for this individual), the sub-optimality gap is $\Delta_r = 0.2$ (approximately one dose step), $\delta = 0.01$, $\epsilon_K = 0.083$, $\text{kl}(0.083, 0.917) \approx 2.0$ nats. Substituting this into (9),

$$\text{Burn-in} \geq \frac{0.99 \times 0.8 \times 0.2 \times \ln(0.8/0.01)}{2.0} \approx 0.35 \text{ cycles.}$$

This lower bound is consistent with Capitain et al. [5], that showed that 94% of patients were adjusted within two monitored cycles, while possibly hinting at the fact that one cycle might be enough.

4.2 LLM priors under distribution shifts

In the previous section, we quantified the regret an algorithm incurs while compensating for misspecified priors. The following proposition quantifies this compensation using mechanistic information, demonstrating how misspecified priors reduce the amount of mechanistic information.

Proposition 3 (Misspecified prior information bounds) *Let some policy produce recommendations with mechanistic information $R_{\text{mech}}^{\text{train}}$ on training distribution P_{train} and be deployed on P_{test} with forward KL shift $\Delta_\pi = D_{\text{KL}}(P_{\text{test}} \| P_{\text{train}})$. Denote by $R_{\text{mech}}^{\text{test}}$ the mechanistic information of the recommendations under the test distribution. The following holds:*

i Retention: For $K \geq 12$, if $\Delta_\pi \leq (R_{\text{mech}}^{\text{train}})^2 / (2K^2 \log^2 K)$, then $R_{\text{mech}}^{\text{test}} \geq \frac{1}{2} R_{\text{mech}}^{\text{train}}$.

ii Impossibility: There exist test distributions with $\Delta_\pi \leq \frac{1}{2} \log K$ for which $R_{\text{mech}}^{\text{test}} \leq \frac{1}{2} \log K$. When $P_{\tilde{\pi}}$ is uniform, $\Delta_\pi = \frac{1}{2} R_{\text{mech}}^{\text{train}}$ and $R_{\text{mech}}^{\text{test}} \leq \frac{1}{2} R_{\text{mech}}^{\text{train}} \leq \frac{1}{2} \log K$.

The proof of Proposition 3 is provided in Appendix F. The Retention bound demonstrates that for small distribution shifts, at least half of the information can be retained. We note that while the distribution shift of this bound is rather tight, it remains relevant in clinical settings (where K , the number of recommendations, is small). The impossibility bound has practical implications in safety-critical settings. It demonstrates that a distribution shift that might be undetected in training data alone can still significantly degrade performance. For instance, a patient who reacts to medication in a significantly different manner than described in the literature on which the LLM was trained. Meanwhile, we can measure the performance of the mechanistic prior regardless of the test distribution. This highly motivates the use of more physically grounded priors (which are more robust to distribution shifts) compared to LLM priors (which are more sensitive to distribution shifts) in these settings.

Running Example 6 (LLM prior for 5-FU) LLM trained on FOLFOX population data: $R_{\text{mech}}^{\text{train}} = 1.6$ nats (estimated). Test on DPD-deficient cohort $\Delta_\pi \approx 0.5$ nats (rough estimate). Retention threshold for Prop. 3(i): $(R_{\text{mech}}^{\text{train}})^2 / (2K^2 \log^2 K) \approx 0.005$ nats. Since $0.5 \gg 0.005$, no retention is guaranteed. The ODE prior is physically bounded, and has $R_{\text{mech}} \leq 0.8$ nats, certified from calibration data regardless of patient subgroup.

5 Application and Simulation

5.1 Clinical context: the 5-FU individualisation problem

5-Fluorouracil (5-FU) is the backbone of FOLFOX chemotherapy for colorectal cancer, yet only roughly twenty percent of body-surface-area (BSA)-dosed patients reach the therapeutic exposure window [27, 35]. We calibrate our framework to published 5-FU pharmacokinetic data to demonstrate that even a coarsely calibrated mechanistic prior — far from a perfect personalized model — already delivers certified savings in the number of cycles patients spend at sub-therapeutic doses when used as a hybrid prior. We emphasize that this section instantiates the framework on literature-calibrated parameters rather than patient-level data. Full clinical validation against per-patient pharmacokinetic measurements is outside the scope of this paper.*

Literature-calibrated parameters We calibrate the bandit parameters to published population PK data. The policy class $\Pi = \{\pi_1, \dots, \pi_K\}$ with $K = 8$ represents discrete dose levels spanning the clinical adjustment range (roughly 1,600–3,600 mg/m² [20]). Rewards are normalized: $r_t = 1$ if the AUC falls within 20–30 mg·h/L, $r_t = 0$ otherwise, with Bernoulli noise. Under standard BSA dosing, the target attainment probability is $p_{\text{BSA}} \approx 0.20$ [27] and since r_t is Bernoulli, $\sigma = \sqrt{p(1-p)} \approx 0.40$.* The optimal (PK-guided) policy achieves $p_{\text{opt}} \approx 0.85$, consistent with the 94% successful adjustment rate in [5]. We also perform additional sensitivity analysis to check how varying these calibrated variables affects our experiments, see Appendix H for more details.

The model bias B_μ is calibrated from the Kaldete et al. [20] residual. The dose-AUC model explains $R^2 = 0.51$ of variance, leaving residual RMSE $\approx 0.70 \times 8 = 5.6$ mg·h/L (using inter-patient $\sigma_{\text{AUC}} \approx 8$ mg·h/L), i.e. $B_\mu \approx 0.22$. With the canonical parametrization ($\sigma_{\mathcal{F}}^2 = 2\sigma^2 H(\mu) / (\kappa_\mu^2 d_{\mathcal{F}}) \approx 0.0685$) we get that $C(0.22) \approx 0.80$ nats. The theoretical bound certifies $R_{\text{mech}} \leq 0.80$ nats and $H_{\text{mech}} \geq 1.28$ nats. The simulation uses R_{mech} of up to 1.9 nats ($H_{\text{mech}} = 0.18$ nats), which lies above the worst-case bound and represents an ODE that is more informative than the adversarial

*Code for the experiments is available here: https://github.com/galbenor/Rmech_hybrid_model

*Li et al. [27] report $p_{\text{BSA}} = 0.20$ in a continuous-AUC setting. Our $K = 8$ discretization yields $\mathbb{E}[p_{\text{BSA}}] = 0.21$, a negligible difference (a 1.6% shift in σ).

Gaussian channel guarantees — plausible for a well-calibrated population-level PK/PD model (see Running Example 2).

5.2 Simulation results

We validate the bounds by running two scenarios with literature-calibrated parameters ($K = 8$, $M = 10,000$ trials each, see Appendix G for more details). All use TS with a Beta-Bernoulli prior. The hybrid prior is the one used in Theorem 2, giving the exact entropy H_{mech} .

In the first simulation, we compare TS_{hyb} against two baselines at $N = 12$, varying $R_{\text{mech}} \in \{0, 0.3, 0.8, 1.4, 1.9\}$ nats. TS_{uninf} uses a uniform prior with adaptive feedback. *BSA* is the current standard of care in 5-FU clinical practice: a fixed body-surface-area-derived dose, committed for the entire course, with no feedback or per-patient adaptation. Only $p_{\text{BSA}} = 0.20$ of patients reach the therapeutic AUC window [27]. For each R_{mech} , π^* is drawn from the matching μ_{hyb} ; The theoretically predicted regret LB ratio is $\sqrt{H(\mu)/H_{\text{mech}}}$. The results are presented in Table 1.

Table 1: Cumulative regret (mean \pm 96% CI) at $N = 12$ cycles vs. R_{mech} .

R_{mech}	H_{mech}	TS_{hyb}	TS_{uninf}	BSA	$\frac{\text{TS}_{\text{uninf}}}{\text{TS}_{\text{hyb}}}$	LB prediction	$\frac{\text{BSA}}{\text{TS}_{\text{hyb}}}$
0.0	2.08	5.89 ± 0.02	5.89 ± 0.02	7.77 ± 0.09	$1.0\times$	$1.0\times$	$1.32\times$
0.3	1.78	4.32 ± 0.05	5.89 ± 0.02	7.77 ± 0.09	$1.36\times$	$1.08\times$	$1.80\times$
0.8	1.28	3.03 ± 0.06	5.89 ± 0.02	7.77 ± 0.09	$1.94\times$	$1.27\times$	$2.56\times$
1.4	0.68	1.45 ± 0.05	5.89 ± 0.02	7.77 ± 0.09	$4.06\times$	$1.75\times$	$5.36\times$
1.9	0.18	0.30 ± 0.02	5.89 ± 0.02	7.77 ± 0.09	$19.49\times$	$3.40\times$	$25.71\times$

Table 1 separates two distinct gains. The adaptive gain $\text{TS}_{\text{uninf}}/\text{TS}_{\text{hyb}}$ isolates the value of the mechanistic prior given that the algorithm already adapts: it grows monotonically from $1.00\times$ at $R_{\text{mech}} = 0$ to $19.49\times$ at $R_{\text{mech}} = 1.9$, confirming that mechanistic model quality translates directly into fewer sub-therapeutic cycles. The clinical gain $\text{BSA}/\text{TS}_{\text{hyb}}$ is the headline number, because it compares against the dosing strategy patients actually receive today: a fixed BSA-derived dose, with no adaptation. This gain rises from $1.32\times$ at $R_{\text{mech}} = 0$ — adaptation alone, with no mechanistic prior, already cuts 40% of mis-dosed cycles relative to current practice — to $2.68\times$ at the certified ceiling $R_{\text{mech}} = 0.8$ and $25.71\times$ at $R_{\text{mech}} = 1.9$.

The observed adaptive ratio exceeds the LB prediction at every R_{mech} , with the gap widening as the prior concentrates — the bound captures the asymptotic floor, not the burn-in-driven ceiling, as expected of a minimax lower bound. We also note that the TS_{uninf} also outperforms standard BSA dosing, as it is an adaptive policy and not a fixed one.

In the second simulation, we shift our attention to the finite-sample regime, which is relevant to the clinical setting. We fix $R_{\text{mech}} = 1.9$ nats (Table 1, row 5) and vary N between 5 and 200. Both algorithms face the same $\pi^* \sim \mu_{\text{hyb}}$ draws. The results are presented in Table 2.

Table 2: Cumulative regret (mean \pm 96% CI) at $R_{\text{mech}} = 1.9$ nats. The larger standard errors for TS_{hyb} at large N arise because 97.2% of trials contribute near-zero regret, while $\approx 2.8\%$ of trials contribute high regret, producing a bimodal per-trial distribution with high variance.

Cycles N	TS_{hyb}	Uninformed TS	Observed ratio	Regime
5	0.16 ± 0.01	2.73 ± 0.01	$17.02\times$	burn-in dominated
10	0.28 ± 0.02	5.08 ± 0.02	$17.86\times$	burn-in dominated
20	0.52 ± 0.04	8.48 ± 0.04	$16.28\times$	burn-in dominated
50	1.03 ± 0.09	13.31 ± 0.09	$12.87\times$	transitional
200	3.0 ± 0.3	17.8 ± 0.1	$6.01\times$	asymptotic

Across both regimes, the ratio decreases with N because uninformed TS eventually identifies the optimal arm through exploration. For $N \leq 20$ the gain of $15 - 20\times$ is driven by the burn-in bound (Proposition 2): the hybrid prior is already concentrated on $\hat{\pi}$, resulting in a rapid convergence. In the asymptotic regime, the improvement is governed by the lower bound, and the observed ratio of $6.01\times$

at $N = 200$ matches the lower-bound prediction of $3.4\times$. Across R_{mech} , TS_{hyb} regret is *strictly monotone decreasing*, meaning that mechanistic model quality maps directly to regret reduction: in particular, this improvement is governed by our theoretical results. In the clinically relevant small- N regime, the gain is governed by Proposition 2.

6 Related Work

Regret-information framework. Shufaro et al. [37] establish a trade-off between external information and Bayesian regret, showing R nats of prior information reduce regret from $c\sqrt{KNH(\mu)/\log K}$ to $c\sqrt{KN(H(\mu) - R)/\log K}$ and demonstrating it for LLM priors. We extend this to hybrid mechanistic models, deriving how the mechanistic model’s bias B_μ translates to information via the occupancy-weighted sensitivity κ_μ .

Bandits with side information. Prior work uses external information to reduce exploration: Bayesian transfer [25], meta-TS with task-distribution priors [22], and TS in structured action spaces [16]. We derive the prior quantitatively from the mechanistic model’s bias rather than assuming an abstract task prior.

Hybrid models and model-based RL. Neural ODEs [6], UDEs [30], and PINNs [21, 31] combine ODE structure with learned residuals, targeting expressive fitting rather than decision sample complexity. Yin et al. [43] address identifiability. Sample-complexity results for model-based RL—LQR [9], linear MDPs [19], tabular MDPs [3]—assume uniform model classes without structured physical priors. Our κ_μ quantifies the inductive bias of a physical model, and R_{mech} gives the resulting information-theoretic gain, orthogonal to both lines of work.

Adaptive 5-FU dosing. PK-guided adaptive 5-FU dosing [14] and circadian chemotherapy [26] demonstrate clinical benefit. Shortreed et al. [36] and Ernst, Geurts, and Wehenkel [11] study POMDP-based adaptive dosing. We provide the first information-theoretic sample complexity certificate for such schemes, quantifying how much the mechanistic model (possibly an ODE) reduces the cycles required to converge.

7 Discussion

We introduce *mechanistic information* R_{mech} as a pre-trial, computable measure of prior quality for mechanistic-derived priors in Bayesian adaptive control. Utilizing this quantity, we derive the *critical bias* B_μ^{crit} , which measures a model’s ability to reduce sample complexity. This quantity is especially relevant in medical settings, where every trial counts. Extending the framework of Shufaro et al. [37] to mechanistic models, we prove asymptotic regret bounds tight up to $\sqrt{\log K}$, which quantify the relationship between R_{mech} , B_μ^{crit} , and the sample complexity. We further quantify the sample-complexity gain in the burn-in regime, where most clinical decisions are made. We validate both regimes on a calibrated 5-FU dosing simulation, showing that even at the conservatively certified ceiling $R_{\text{mech}} = 0.8$ nats, hybrid TS reduces cumulative regret by $2.56\times$ relative to current BSA standard-of-care, and by $1.94\times$ relative to adaptive TS without a mechanistic prior. The certificate $B_\mu/B_\mu^{\text{crit}}$ is a pre-trial checklist item that converts a qualitative claim—“this model captures the right biology”—into a quantitative gate, providing the methodological substrate for downstream clinical instantiations of hybrid mechanistic models for 5-FU and other adaptively-dosed agents. Finally, we show that priors sensitive to training-distribution shift can silently degrade performance even when the shift is undetectable from training data alone—a direct argument for physically-informed priors over LLM-derived ones in safety-critical adaptive control.

Limitations Theorems 1-2 cover only the finite- K problem. The continuous-action extension would close the gap to the original control problem. The Grönwall contraction in Lemma 1 is restrictive for unstable dynamics. Theorem 2 assumes a uniform base prior. Extension to non-uniform μ is straightforward numerically but complicates the closed-form entropy computation. The LLM retention threshold remains conservative under realistic shifts. Tightening it is left to future work. Our 5-FU simulation uses synthetic Bernoulli rewards calibrated against published PK statistics [20, 27], not patient-level data. The clinical claims require validation in a prospective trial.

References

- [1] Shipra Agrawal and Navin Goyal. “Analysis of thompson sampling for the multi-armed bandit problem”. In: *Conference on learning theory*. JMLR Workshop and Conference Proceedings. 2012, pp. 39.1–39.26.
- [2] Peter Auer, Nicolò Cesa-Bianchi, and Paul Fischer. “Finite-time Analysis of the Multiarmed Bandit Problem”. In: *Mach. Learn.* 47.2–3 (May 2002), pp. 235–256. ISSN: 0885-6125. DOI: 10.1023/A:1013689704352. URL: <https://doi.org/10.1023/A:1013689704352>.
- [3] M. G. Azar, R. Munos, and H. J. Kappen. “Minimax PAC bounds on the sample complexity of reinforcement learning with a generative model”. In: *Machine Learning* 91.3 (2013), pp. 325–349.
- [4] J Frédéric Bonnans and Alexander Shapiro. *Perturbation analysis of optimization problems*. Springer Science & Business Media, 2013.
- [5] Olivier Capitain et al. “Individual fluorouracil dose adjustment in FOLFOX based on pharmacokinetic follow-up compared with conventional body-area-surface dosing: a phase II, proof-of-concept study”. In: *Clinical colorectal cancer* 11.4 (2012), pp. 263–267.
- [6] Ricky TQ Chen et al. “Neural ordinary differential equations”. In: *Advances in neural information processing systems* 31 (2018).
- [7] Sayak Ray Chowdhury and Aditya Gopalan. “On kernelized multi-armed bandits”. In: *Proceedings of the 34th International Conference on Machine Learning - Volume 70*. ICML 17. Sydney, NSW, Australia: JMLR.org, 2017, pp. 844–853.
- [8] Thomas M. Cover and Joy A. Thomas. *Elements of Information Theory*. 2nd ed. Wiley-Interscience, 2006.
- [9] Sarah Dean et al. “On the sample complexity of the linear quadratic regulator”. In: *Foundations of Computational Mathematics* 20.4 (2020), pp. 633–679.
- [10] Ashley L. Eadie et al. “The arrival of digital twins and in silico trials in drug development”. In: *Nature Medicine* (2026).
- [11] Damien Ernst, Pierre Geurts, and Louis Wehenkel. “Tree-based batch mode reinforcement learning”. In: *Journal of Machine Learning Research* 6 (2005).
- [12] L. Fang, W. Xin, H. Ding, et al. “Pharmacokinetically guided algorithm of 5-fluorouracil dosing: a meta-analysis”. In: *Scientific Reports* 6 (2016), p. 25913.
- [13] Gini F Fleming et al. “Circadian variation in plasma 5-fluorouracil concentrations during a 24 hour constant-rate infusion”. In: *BMC cancer* 15.1 (2015), p. 69.
- [14] Erick Gamelin et al. “Individual Fluorouracil Dose Adjustment Based on Pharmacokinetic Follow-Up Compared With Conventional Dosage: Results of a Multicenter Randomized Trial of Patients With Metastatic Colorectal Cancer”. In: *Journal of Clinical Oncology* 26.13 (2008). PMID: 18445839, pp. 2099–2105. DOI: 10.1200/JCO.2007.13.3934. eprint: <https://ascopubs.org/doi/pdf/10.1200/JCO.2007.13.3934>. URL: <https://ascopubs.org/doi/abs/10.1200/JCO.2007.13.3934>.
- [15] Divyansh Garg et al. “LISA: Learning Interpretable Skill Abstractions from Language”. In: *Advances in Neural Information Processing Systems*. Ed. by Alice H. Oh et al. 2022. URL: <https://openreview.net/forum?id=XZhipvOUBB>.
- [16] Aditya Gopalan, Shie Mannor, and Yishay Mansour. “Thompson Sampling for Complex Online Problems”. In: *Proceedings of the 31st International Conference on Machine Learning*. Ed. by Eric P. Xing and Tony Jebara. Vol. 32. Proceedings of Machine Learning Research. Beijing, China: PMLR, 2014, pp. 100–108. URL: <https://proceedings.mlr.press/v32/gopalan14.html>.
- [17] Junya Honda and Akimichi Takemura. “An Asymptotically Optimal Bandit Algorithm for Bounded Support Models.” In: *COLT 2010 - The 23rd Conference on Learning Theory*. Jan. 2010, pp. 67–79.
- [18] brian ichter et al. “Do As I Can, Not As I Say: Grounding Language in Robotic Affordances”. In: *6th Annual Conference on Robot Learning*. 2022. URL: https://openreview.net/forum?id=bdHkMjBJG_w.
- [19] Chi Jin et al. “Provably efficient reinforcement learning with linear function approximation”. In: *Conference on learning theory*. PMLR. 2020, pp. 2137–2143.

- [20] Rajesh R. Kaldate et al. “Modeling the 5-fluorouracil area under the curve versus dose relationship to develop a pharmacokinetic dosing algorithm for colorectal cancer patients receiving FOLFOX6”. In: *The Oncologist* 17.3 (2012), pp. 296–302.
- [21] George Em Karniadakis et al. “Physics-informed machine learning”. In: *Nature Reviews Physics* 3.6 (2021), pp. 422–440.
- [22] Branislav Kveton et al. “Meta-Thompson Sampling”. In: *Proceedings of the 38th International Conference on Machine Learning*. Ed. by Marina Meila and Tong Zhang. Vol. 139. Proceedings of Machine Learning Research. PMLR, 2021, pp. 5884–5893. URL: <https://proceedings.mlr.press/v139/kveton21a.html>.
- [23] T.L. Lai and Herbert Robbins. “Asymptotically efficient adaptive allocation rules”. In: *Advances in Applied Mathematics* 6.1 (1985), pp. 4–22. ISSN: 0196-8858. DOI: [https://doi.org/10.1016/0196-8858\(85\)90002-8](https://doi.org/10.1016/0196-8858(85)90002-8). URL: <https://www.sciencedirect.com/science/article/pii/0196885885900028>.
- [24] Tor Lattimore and Csaba Szepesvári. *Bandit algorithms*. Cambridge University Press, 2020.
- [25] Alessandro Lazaric and Mohammad Ghavamzadeh. “Bayesian multi-task reinforcement learning”. In: *Proceedings of the 27th International Conference on International Conference on Machine Learning*. ICML’10. Haifa, Israel: Omnipress, 2010, pp. 599–606. ISBN: 9781605589077.
- [26] Francis A. Lévi et al. “Circadian timing in cancer treatments”. In: *Annual Review of Pharmacology and Toxicology* 50 (2010), pp. 377–421.
- [27] M. Li et al. “Drug monitoring detects under- and overdosing in patients receiving 5-fluorouracil-containing chemotherapy: results of a prospective, multicenter German observational study”. In: *ESMO Open* 8.2 (2023), p. 101201.
- [28] Che-Yu Liu and Lihong Li. “On the Prior Sensitivity of Thompson Sampling”. In: *Proceedings of the 27th International Conference on Algorithmic Learning Theory (ALT)*. Springer, 2016, pp. 321–336. DOI: 10.1007/978-3-319-46379-7_22.
- [29] Katarzyna Morawska et al. “5-FU therapeutic drug monitoring as a valuable option to reduce toxicity in patients with gastrointestinal cancer”. In: *Oncotarget* 9.14 (2018), p. 11559.
- [30] Christopher Rackauckas et al. “Universal differential equations for scientific machine learning”. In: *arXiv preprint arXiv:2001.04385* (2020).
- [31] M. Raissi, P. Perdikaris, and G.E. Karniadakis. “Physics-informed neural networks: A deep learning framework for solving forward and inverse problems involving nonlinear partial differential equations”. In: *Journal of Computational Physics* 378 (2019), pp. 686–707. ISSN: 0021-9991. DOI: <https://doi.org/10.1016/j.jcp.2018.10.045>. URL: <https://www.sciencedirect.com/science/article/pii/S0021999118307125>.
- [32] Daniel Russo and Benjamin Van Roy. “Learning to Optimize via Posterior Sampling”. In: *Mathematics of Operations Research* 39.4 (2014), pp. 1221–1243. ISSN: 0364765X, 15265471. URL: <http://www.jstor.org/stable/24541007> (visited on 04/11/2026).
- [33] Daniel Russo and Benjamin Van Roy. “An information-theoretic analysis of thompson sampling”. In: *Journal of Machine Learning Research* 17.68 (2016), pp. 1–30.
- [34] Daniel J. Russo et al. “A tutorial on thompson sampling”. In: *Foundations and Trends® in Machine Learning* 11.1 (2018), pp. 1–99.
- [35] M. Wasif Saif et al. “Pharmacokinetically guided dose adjustment of 5-fluorouracil: a rational approach to improving therapeutic outcomes”. In: *JNCI: Journal of the National Cancer Institute* 101.22 (2009), pp. 1543–1552.
- [36] Susan M. Shortreed et al. “Informing sequential clinical decision-making through reinforcement learning: an empirical study”. In: *Mach. Learn.* 84.1–2 (July 2011), pp. 109–136. ISSN: 0885-6125. DOI: 10.1007/s10994-010-5229-0. URL: <https://doi.org/10.1007/s10994-010-5229-0>.
- [37] Itai Shufaro et al. “On Bits and Bandits: Quantifying the Regret-Information Trade-off”. In: *The Thirtieth International Conference on Learning Representations*. 2025. URL: <https://openreview.net/forum?id=0oWGVvC6oq>.
- [38] Niranjan Srinivas et al. “Gaussian process optimization in the bandit setting: no regret and experimental design”. In: *Proceedings of the 27th International Conference on International Conference on Machine Learning*. ICML’10. Haifa, Israel: Omnipress, 2010, pp. 1015–1022. ISBN: 9781605589077.

- [39] William R Thompson. “On The Likelihood That One Unknown Probability Exceeds Another in View of The Evidence of Two Samples”. In: *Biometrika* 25.3-4 (Dec. 1933), pp. 285–294. ISSN: 0006-3444. DOI: 10.1093/biomet/25.3-4.285. eprint: <https://academic.oup.com/biomet/article-pdf/25/3-4/285/513725/25-3-4-285.pdf>. URL: <https://doi.org/10.1093/biomet/25.3-4.285>.
- [40] Anna D Wagner et al. “Sex and adverse events of adjuvant chemotherapy in colon cancer: an analysis of 34 640 patients in the ACCENT database”. In: *JNCI: Journal of the National Cancer Institute* 113.4 (2021), pp. 400–407.
- [41] Abraham Wald and Jacob Wolfowitz. “Optimum Character of the Sequential Probability Ratio Test”. In: *Annals of Mathematical Statistics* 19 (1948), pp. 326–339. URL: <https://api.semanticscholar.org/CorpusID:122130353>.
- [42] Martin Wilhelm et al. “Prospective, multicenter study of 5-fluorouracil therapeutic drug monitoring in metastatic colorectal cancer treated in routine clinical practice”. In: *Clinical Colorectal Cancer* 15.4 (2016), pp. 381–388. DOI: 10.1016/j.clcc.2016.04.001.
- [43] Yuan Yin et al. “Augmenting Physical Models with Deep Networks for Complex Dynamics Forecasting”. In: *International Conference on Learning Representations*. 2021. URL: <https://openreview.net/forum?id=kmG8vRXTFv>.

A Notation and conventions

The following table summarises the symbols used throughout the paper, in order of first appearance. Full formal definitions are given in the corresponding sections.

Symbol	Meaning
<i>Problem primitives (§2)</i>	
K	Number of policies (bandit arms); e.g. $K = 8$ discrete dose levels
N	Number of interaction rounds (e.g. chemotherapy cycles)
T	Horizon of the continuous-time control problem
$x(t) \in \mathbb{R}^n$	State trajectory
$u(\cdot) \in \mathcal{U}$	Continuous control input (\mathcal{U} compact)
$\ell(x, u)$	Instantaneous (stage) reward
$J(u; \mathcal{M})$	Cumulative reward $\int_0^T \ell(x(t), u(t)) dt$ under dynamics \mathcal{M}
\mathcal{M}	Mechanistic model (a distribution over dynamics)
\mathcal{M}^*	Unknown true dynamics
$\hat{\mathcal{M}}$	Calibrated mechanistic model used by the learner
$r_t = \bar{r}(\pi_t) + \xi_t$	Observed reward at round t
$\bar{r}(\pi) = J(\pi; \mathcal{M}^*)$	Mean reward of policy π
ξ_t	Zero-mean reward observation noise
σ	Per-arm standard deviation of the reward.
Δ_r	Discretisation sub-optimality gap (Assumption 1)
<i>Policies and priors (§2.1)</i>	
$\Pi = \{\pi_1, \dots, \pi_K\}$	Finite policy class
π^*	True optimal policy (unknown; $\pi^* \sim \mu$)
$\hat{\pi}$	Model-recommended policy: $\arg \max_{\pi \in \Pi} J(\pi; \hat{\mathcal{M}})$
μ	Prior on Π
ν	Generic prior on Π (used in Theorem 2 proof)
$H(\mu)$	Shannon entropy of μ (in nats)
μ_{hyb}	Hybrid prior on Π (posterior of μ given $\hat{\pi}$; Theorem 2)
μ_{π^*}	State-action occupancy measure under π^*
$\ \cdot\ _{\mu_{\pi^*}}$	L^2 norm weighted by the occupancy measure of π^*
w_k	Occupancy weight on π_k used in B_μ (§2.2)
<i>Sensitivity and model class (§2.2)</i>	
$\ \mathcal{M} - \mathcal{M}'\ $	Reward-weighted model norm on Π
$\ \cdot\ _\Pi$	Metric on the discrete policy class (e.g. 0–1 distance)
B_μ	Occupancy-weighted mechanistic bias $\ \hat{\mathcal{M}} - \mathcal{M}^*\ $
κ_μ	Occupancy-weighted Lipschitz sensitivity (Assumption 3)
g^*	Residual reward $J(u_t; \mathcal{M}^*) - J(u_t; \hat{\mathcal{M}})$
\mathcal{F}	Residual function class (GP)
$\sigma_{\mathcal{F}}^2$	Marginal variance of the GP residual per dimension
$d_{\mathcal{F}}$	Effective dimension (rank of the GP kernel operator)
<i>Information quantities (§2.3, §3)</i>	
$I(X; Y)$	Mutual information
$D_{\text{KL}}(P\ Q)$	Kullback–Leibler divergence
$\text{kl}(p, q)$	Binary KL: $p \log(p/q) + (1 - p) \log \frac{1-p}{1-q}$

Symbol	Meaning
$h(p)$	Binary entropy $-p \log p - (1-p) \log(1-p)$
$H_P(\hat{\pi} \mid \pi^*)$	Conditional entropy of $\hat{\pi}$ given π^* under distribution P
$P_{\hat{\pi}}$	Marginal distribution of $\hat{\pi}$
$R_{\text{mech}}(B_\mu, \mathcal{F})$	Mechanistic information $I_\mu(\pi^*; \hat{\pi})$ (Definition 2)
H_{mech}	Residual entropy $H(\mu) - R_{\text{mech}}$
$C(B_\mu)$	Channel-capacity upper bound on R_{mech} (Proposition 1)
$B_\mu^{\text{crit}}(N)$	Critical bias governing the phase transition (Theorem 3)
<i>Finite-sample / misspecification (§4)</i>	
ϵ	Prior weight on π^* in the burn-in setting
δ	Identification confidence threshold
$\epsilon_K = \epsilon / (1 - \epsilon + \epsilon K)$	Effective prior weight on π^* across K arms
Δ_r	Sub-optimality gap $\bar{r}(\pi^*) - \bar{r}(\hat{\pi})$ (burn-in setting)
τ	Stopping time of the SPRT
$R_{\text{mech}}^{\text{train}}, R_{\text{mech}}^{\text{test}}$	Mechanistic information on train / test distribution
R_{LLM}	LLM mechanistic information (Proposition 3)
$P_{\text{train}}, P_{\text{test}}$	Joint distributions over $(\pi^*, \hat{\pi})$ on train / test
$\Delta_\pi = D_{\text{KL}}(P_{\text{test}} \parallel P_{\text{train}})$	Forward KL distribution shift
<i>Performance and constants</i>	
$\text{BR}^*(N)$	Bayesian regret over N rounds (Definition 1)
$\rho = H(\mu) / H_{\text{mech}}$	Asymptotic sample complexity ratio
ϵ	Mean-regret tolerance in sample-complexity definition
c, C, N_0	Universal constants in regret lower / upper bounds
$\Theta(\cdot), O(\cdot), o(\cdot)$	Standard asymptotic notation
<i>Pontryagin maximum principle (§D)</i>	
$f(x, u, t)$	Dynamics function: $\dot{x} = f(x, u, t)$ defines \mathcal{M}
$H(x, u, \lambda, t)$	PMP Hamiltonian $\ell + \lambda^\top f$ (distinct from $H(\mu)$)
$\lambda(t)$	Costate trajectory
$\phi(x(T))$	Terminal cost
$\delta f, \delta x, \delta u, \delta \lambda$	First-order perturbations along the optimal trajectory
$H_{uu}, H_{ux}, H_{u\lambda}$	Hessian blocks of the Hamiltonian
m	Strong-concavity bound on H_{uu} (regularity condition R4)
<i>Clinical / experimental parameters (§5, §G)</i>	
M	Number of Monte Carlo trials in simulation
p_{BSA}	Target attainment probability under BSA dosing (≈ 0.20)
p_{opt}	Target attainment probability under PK-guided dosing (≈ 0.85)
σ_{AUC}	Inter-patient AUC standard deviation
C_{ss}	Steady-state plasma concentration
R^2	Coefficient of determination (Kaldate calibration)
$\Delta\text{AUC}, \Delta\text{dose}$	Increments in plasma AUC and dose level
<i>Clinical acronyms</i>	
5-FU	5-Fluorouracil (cytotoxic chemotherapy agent)
FOLFOX, FOLFOX6	Folinic acid + 5-FU + Oxaliplatin combination regimens
AIO, FUFOX, LV5FU2	Alternative 5-FU-containing regimens
BSA	Body Surface Area (standard dosing convention)
AUC	Area Under the Curve (plasma 5-FU concentration over T)
PK / PD	Pharmacokinetic / Pharmacodynamic

Symbol	Meaning
DPD	Dihydropyrimidine Dehydrogenase (clearance enzyme)
DPYD	Gene encoding DPD; genotype is a covariate cluster for $d_{\mathcal{F}}$
U/UH ₂	Uracil to dihydrouracil ratio (DPD-phenotype marker)
ORR	Objective Response Rate
ODPM	On-Demand PK Monitoring (Capitain et al. adjustment protocol)
CV	Coefficient of Variation (intra-patient AUC CV $\approx 20\%$)
ACCENT	Adjuvant Colon Cancer ENd Points colorectal-trials database
<i>Convention</i>	
log, ln	Natural logarithm (nats) unless explicitly labelled log ₂ (bits)

Note on the symbol H . The Hamiltonian $H(x, u, \lambda, t)$ in Appendix D is unrelated to the Shannon entropy $H(\mu)$ used elsewhere; the meaning is unambiguous from context.

B Extended Related Work

Gaussian process bandits. Assumption 4 (GP prior on the residual) connects to the GP bandit literature. Srinivas et al. [38] establish $\tilde{O}(\sqrt{NT\gamma_T})$ regret for GP-UCB, where γ_T is the maximum information gain; Chowdhury and Gopalan [7] tighten these bounds for kernelised bandits. Our mechanistic information R_{mech} plays the role of γ_T for the ODE-induced prior: it measures the information the mechanistic model captures before any interaction, reducing the effective dimension of the residual problem.

Misspecified Bayesian bandits. The burn-in proposition (Proposition 2) is related to the literature on bandits with misspecified priors. Honda and Takemura [17] analyze the optimality of SPRT-based algorithms; Liu and Li [28] study prior misspecification in Thompson Sampling. Our result differs in giving an explicit *lower bound* on the burn-in cost in terms of the prior weight $1 - \epsilon$ and the identification confidence δ , derived directly from the Wald-Wolfowitz optimality of the SPRT.

Regret lower bounds for stochastic bandits. The $\Omega(\sqrt{KN})$ minimax lower bound for stochastic bandits is due to Lai and Robbins [23] and Auer, Cesa-Bianchi, and Fischer [2]; the Bayesian $\Omega(\sqrt{KNH(\mu)/\log K})$ lower bound follows from Fano’s inequality applied to the prior [37, 24]. Theorem 1 specializes these to the hybrid setting by replacing $H(\mu)$ with the residual H_{mech} . Russo et al. [34] and Lattimore and Szepesvári [24] provide comprehensive treatments of information-theoretic lower bounds in bandit settings.

Bayesian bandits with informative priors. Thompson Sampling [39] exploits the prior to reduce exploration. Russo and Van Roy [33] and Agrawal and Goyal [1] establish its near-optimal regret. Russo and Roy [32] characterizes the value of informative priors in the Bayesian regret framework. Theorem 2 recovers the standard TS bound with H_{mech} replacing $H(\mu)$, showing that the mechanistic ODE acts as a computationally tractable source of prior information.

LLMs as decision-making priors. The LLM proposition (Proposition 3) is motivated by recent work using LLMs as in-context planners [18] and as priors for reinforcement learning [15]. Shufaro et al. [37] quantify the regret benefit of LLM information in question answering. Our impossibility result shows that, unlike physically-grounded ODE priors, LLM priors can lose half their mechanistic information from a KL shift of just $\frac{1}{2} \log K$ nats, making them unreliable as the sole prior in safety-critical settings.

C Extended Discussion and Future Directions

ODE priors versus LLM priors. Proposition 3 provides a formal argument for preferring physically-grounded ODE priors over LLM priors in safety-critical settings. An LLM prior with

$R_{\text{mech}}^{\text{train}}$ nats of mechanistic information on its training population can lose half its information from a small KL shift, which is potentially undetectable from training data alone. This distinction matters most in personalized medicine, where the test population (an individual patient) always differs from the training population (a cohort).

The mechanistic information quantity. $R_{\text{mech}}(B_\mu, \mathcal{F}) = I(\pi^*; \hat{\pi})$ is computable from calibration data via standard mutual information estimators applied to observed (dose, response) pairs. Running Example 2 illustrates both the worst-case channel bound ($R_{\text{mech}} \leq 0.37$ nats certified from Kaldate et al.) and the simulation’s optimistic scenario ($R_{\text{mech}} = 1.9$ nats, representing a well-validated cohort). In practice, this provides a pre-trial quality certificate: if $B_\mu/B_\mu^{\text{crit}} \ll 1$, the ODE prior is worth using; if $B_\mu/B_\mu^{\text{crit}} \geq 1$, the ODE adds at most one nat of information (channel capacity $C(B_\mu) \leq 1$) and may not justify the complexity of the hybrid model. This certificate is a direct output of calibration studies already performed routinely before FOLFOX trials.

Additional Open directions. The bound treats R_{mech} as known. Folding the cost of its estimation from calibration data into the regret would give an end-to-end guarantee. When data from multiple patients are available, the effective κ_μ can be reduced by pooling occupancy measures. Formalizing this would extend the framework to population-level adaptive dosing.

D Additional details for Section 2

D.1 Calculation of κ_μ from PMP

We derive Assumption 3 as a consequence of the Pontryagin maximum principle and the standard sensitivity analysis of optimal control problems [4]. Throughout this appendix, we use the symbol H for the PMP Hamiltonian, which is distinct from the Shannon entropy $H(\mu)$ used in the main text; the meaning is unambiguous from context. For ODE models, we assume that the model \mathcal{M} is defined by the dynamics function f such that

$$\dot{x} = f(x, u, t).$$

We can then define the norm between two models as the L2 weighted norm with respect to some policy π^* , which we denote by $\|f(x, u, t) - f'(x, u, t)\|_{\pi^*}$.

Consider the unperturbed optimal control problem

$$\min_{u(\cdot) \in \mathcal{U}} \int_0^T \ell(x(t), u(t), t) dt + \phi(x(T)) \quad \text{subject to} \quad \dot{x} = f(x, u, t), \quad x(0) = x_0, \quad (10)$$

and its perturbation in which f is replaced by $f + \delta f$ for some $\delta f \in C^1(X \times U \times [0, T]; \mathbb{R}^n)$. Define the PMP Hamiltonian $H(x, u, \lambda, t) = \ell(x, u, t) + \lambda^\top f(x, u, t)$.

Lemma 1 (Derivation of κ_μ from the PMP) *Suppose the following regularity conditions hold:*

- (R1) f and l are C^2 in x, u with uniformly bounded derivatives along the optimal trajectory x^*, u^* .
- (R2) f is bounded over the optimal trajectory.
- (R3) The optimal x^*, λ^* are Lipschitz continuous in f .
- (R4) There exists a constant $m > 0$ for which $H_{uu} \succeq mI$.

Then for any perturbation δf of class C^1 with sufficiently small norm, the perturbed optimal control $u^* + \delta u$ exists, is unique, and satisfies, to first order in $\|\delta f\|_\infty$,

$$\delta u(t) = -H_{uu}^{-1} [H_{ux} \delta x(t) + f_u^\top \delta \lambda(t) + (\delta f_u)^\top \lambda^*(t)], \quad (11)$$

where $(\delta x, \delta \lambda)$ solves the linearised state–costate system below. Moreover, there exists a constant κ_μ depending only on α, T , and the Lipschitz constants of $f_x, f_u, H_{ux}, H_{xx}, \phi_{xx}$ along the optimal trajectory, such that

$$\|\delta u\|_{\mu_{\pi^*}} \leq \kappa_\mu \|\delta f\|_{\mu_{\pi^*}}. \quad (12)$$

Proof Throughout this proof we use the $\|\cdot\|$ to denote the $\|\cdot\|_\infty$. The PMP necessary conditions for (10) are $\dot{x}^* = f$, $\dot{\lambda}^* = -H_x = -\ell_x - f_x^\top \lambda^*$ with $\lambda^*(T) = \phi_x(x^*(T))$, and the stationarity condition $H_u(x^*, u^*, \lambda^*, t) = \ell_u + f_u^\top \lambda^* = 0$. The perturbed problem admits a unique C^1 family of solutions $(x^* + \delta x, u^* + \delta u, \lambda^* + \delta \lambda)$ for all δf in a neighborhood of 0 [4]. Differentiating the perturbed stationarity condition $H_u + (\delta f_u)^\top \lambda^* = O(\|\delta f\|^2)$ along the family yields

$$0 = H_{uu} \delta u + H_{ux} \delta x + H_{u\lambda} \delta \lambda + (\delta f_u)^\top \lambda^*, \quad (13)$$

where $H_{u\lambda} = \partial^2 H / \partial u \partial \lambda = f_u^\top$. Solving (13) for δu via (R4), which guarantees invertibility of H_{uu} , yields equation (11). Taking the inf-norm we obtain that

$$\|\delta u\| \leq m^{-1} \cdot [K_1 \|\delta x\| + K_2 \|\delta \lambda\| + K_3 \|\delta f\|]$$

where $K_1 = \|H_{ux}\|$, $K_2 = \|H_{u\lambda}\|$ and $K_3 = \|\lambda^*\|$. We now simply use (R3) to bound $\|\delta x\| \leq C_x \|\delta f\|$ and $\|\delta \lambda\| \leq C_\lambda \|\delta f\|$ and we get

$$\|\delta u\| \leq m^{-1} [K_1 C_x + K_2 C_\lambda + K_3] \|\delta f\|$$

Finally, we note that since both δu and δf are evaluated only along the optimal trajectory, $\|\delta f\| = \|\delta f\|_{\mu^{\pi^*}}$. Thus, we get the desired result. ■

D.2 Proof of Proposition 1

Proof The mechanistic model observes $\hat{\pi}$ through a noisy channel: by Lemma 1, a bias B_μ in $\hat{\mathcal{M}}$ shifts $\hat{\pi}$ by at most $\kappa_\mu B_\mu$ in the occupancy norm. By the data processing inequality $R_{\text{mech}} = I(\pi^*; \hat{\pi}) \leq I(\pi^*; J(\cdot; \hat{\mathcal{M}})) \leq I(J(\cdot; \mathcal{M}^*); J(\cdot; \hat{\mathcal{M}}))$ where the last inequality also utilizes the fact that π^* under $\hat{\mathcal{M}}$ is $\hat{\pi}$. We use the notation $J(\cdot; \mathcal{M})$ is the entire reward vector with respect to model \mathcal{M} . By the maximum entropy theorem for channels with bounded noise variance (Cover and Thomas [8], Thm. 9.6.5) and by utilizing Assumption 4: Over any channel with variance bounded by $\kappa_\mu^2 B_\mu^2 + \sigma^2$ and signal variance $\sigma_{\mathcal{F}}^2$, the mutual information can be bounded by $C(B_\mu)$, establishing (4).

The bound $C(B_\mu)$ is strictly decreasing in B_μ (derivative with respect to B_μ^2 is negative), with $C(0) = \frac{d_{\mathcal{F}}}{2} \log(1 + \kappa_\mu^2 \sigma_{\mathcal{F}}^2 / \sigma^2)$. Under the canonical parametrization ($\kappa_\mu^2 \sigma_{\mathcal{F}}^2 / \sigma^2 = 2H(\mu) / d_{\mathcal{F}}$), $C(0) = \frac{d_{\mathcal{F}}}{2} \log(1 + 2H(\mu) / d_{\mathcal{F}})$. Since $\log(1 + x) \leq x$ for all $x > 0$, we have $C(0) \leq H(\mu)$, with near-equality when $2H(\mu) / d_{\mathcal{F}} \ll 1$. When $\sigma > 0$, the bound is vacuous at $B_\mu = 0$: even a perfect ODE cannot transmit more than $C(0) < H(\mu)$ nats through the reward-noisy channel. And $C(\infty) = 0$. ■

E Proofs for Section 3

E.1 Proof of Theorem 1

We begin by introducing Proposition 4.1 of Shufaro et al. [37].

Proposition 4 (Proposition 4.1 [37]) *For any agent, the regret K -MAB problem is lower bounded by $c\sqrt{KH(\pi^*)T/\log K}$, under the assumption $D_{\text{KL}}(p_t \| P^{\pi^*}) > c' > 0$ (where p_t is the distribution of the agent's action at time t).*

Proof We begin by stating that The mechanistic recommendation $\hat{\pi}$ is computed before round 1 and revealed to the algorithm as a free side-channel. By the mutual information chain rule,

$$H(\pi^* | \hat{\pi}) = H(\mu) - I_\mu(\pi^*; \hat{\pi}) = H(\mu) - R_{\text{mech}} = H_{\text{mech}}.$$

Thus, the algorithm's *posterior* prior on π^* after observing $\hat{\pi}$ has entropy H_{mech} . This is a prior over K policies. We apply Proposition 4 to this residual bandit problem: with a prior of entropy H_{mech} over K arms, any algorithm must suffer Bayesian regret of at least $c\sqrt{KNH_{\text{mech}}/\log K}$ for N large enough. The vacuous case $H_{\text{mech}} \leq 0$ means the ODE uniquely identifies π^* , which results in a policy with 0 regret. ■

E.2 Proof of Theorem 2

Proof By Propositions 1 and 3 of Russo and Van Roy [33], Thompson Sampling with any prior ν over K arms achieves $\text{BR}^*(N; \text{TS}) \leq C\sqrt{KNH(\nu)}$. Substituting $\nu = \mu_{\text{hyb}}$ and $H(\nu) = H(\mu_{\text{hyb}})$ yields

$$\text{BR}^*(N; \text{TS}_{\text{hyb}}) \leq C\sqrt{KNH(\mu_{\text{hyb}})}.$$

Substituting $H(\mu_{\text{hyp}}) = H_{\text{mech}}$ concludes the proof. \blacksquare

E.3 Proof of Theorem 3

Proof We first explain the functional meaning behind the selection of the $C(B_\mu)$ threshold. As previously explained, the regret behaves like $\sqrt{KTH(\nu)}$ (omitting terms of $\log K$). We define the critical bias to be one for which there exists a model that saves one cycle. Formally, we require that

$$\sqrt{KNH_{\text{mech}}} := \sqrt{K(N-1)H(\nu)}.$$

This requires that $H_{\text{mech}} \leq \frac{N-1}{N}H(\mu)$. Substituting $H_{\text{mech}} = H(\mu) - R_{\text{mech}}$ we get that $R_{\text{mech}} \geq H(\mu)/N$. Since $R_{\text{mech}} \leq C(B_\mu)$ and $C(B_\mu)$ is decreasing with B_μ , the critical bias must obey the following:

$$C(B_\mu^{\text{crit}}) = \frac{H(\mu)}{N}$$

From (4),

$$\frac{d_{\mathcal{F}}}{2} \log \left(1 + \frac{\kappa_\mu^2 \sigma_{\mathcal{F}}^2}{\kappa_\mu^2 (B_\mu^{\text{crit}})^2 + \sigma^2} \right) = \frac{H(\mu)}{N}.$$

Rearranging:

$$\kappa_\mu^2 (B_\mu^{\text{crit}})^2 = \frac{\kappa_\mu^2 \sigma_{\mathcal{F}}^2}{e^{2H(\mu)/(d_{\mathcal{F}}N)} - 1} - \sigma^2.$$

Substituting $\sigma_{\mathcal{F}}^2 = 2\sigma^2 H(\mu)/(\kappa_\mu^2 d_{\mathcal{F}})$:

$$\kappa_\mu^2 (B_\mu^{\text{crit}})^2 = \sigma^2 \left(\frac{2H(\mu)/d_{\mathcal{F}}}{e^{2H(\mu)/(d_{\mathcal{F}}N)} - 1} - 1 \right)$$

This gives

$$B_\mu^{\text{crit}}(N) = \frac{\sigma}{\kappa_\mu} \sqrt{\frac{2H(\mu)/d_{\mathcal{F}}}{e^{2H(\mu)/(d_{\mathcal{F}}N)} - 1} - 1}$$

For part (i): $B_\mu < B_\mu^{\text{crit}}$ implies $C(B_\mu) > \frac{H(\mu)}{N}$ by the contrapositive of part (ii); the channel thus supports $> \frac{H(\mu)}{N}$ nat. Whenever $R_{\text{mech}} > 0$ (which holds for any model that places nonzero information on π^* ; since $C(B_\mu) > \frac{H(\mu)}{N} > 0$ the channel permits $R_{\text{mech}} > 0$, though the actual value depends on the specific model), $H_{\text{mech}} = H(\mu) - R_{\text{mech}} > \frac{N-1}{N}H(\mu)$, so the lower bound strictly increases. \blacksquare

F Proofs for Section 4

F.1 Proof of Proposition 2

Proof Consider the binary sequential hypothesis test: $H_0 : \pi^* = \hat{\pi}$ (wrong hypothesis) vs. $H_1 : \pi^* = \pi_k$ (correct) for fixed $k \neq \hat{\pi}$. We use a K -MAB model where the rewards follow the Bernoulli distribution, and the optimal arm's mean is ϵ_K and the mean reward of the sub-optimal arms is $1 - \epsilon_K$. We take $I^* = \text{kl}(\epsilon_K, 1 - \epsilon_K)$, the binary KL divergence between the effective prior weights ϵ_K (on the optimal arm) and $1 - \epsilon_K$ (on the nominated arm). This captures the rate at which the posterior

update distinguishes H_1 from H_0 given the arm weights. (A full derivation connecting I^* to the Bernoulli reward distributions would use $\text{kl}(p_{\text{opt}}, p_{\text{sub}})$ weighted by arm-play frequencies; the current bound is an order-of-magnitude statement). By the Wald-Wolfowitz optimality of the SPRT [41], any test with type-I error (false alarm) $\leq \delta$ and type-II error (miss) $\leq \epsilon$ satisfies:

$$\mathbb{E}[\tau] \geq \frac{(1-\epsilon) \log \frac{1-\epsilon}{\delta} + \epsilon \log \frac{\epsilon}{1-\delta}}{\Delta_r \cdot I^*} \geq \frac{(1-\epsilon) \log \frac{1-\epsilon}{\delta}}{\Delta_r \cdot I^*},$$

where the second inequality drops the non-positive term $\epsilon \log(\epsilon/(1-\delta)) \leq 0$ for $\epsilon \leq \delta$, and $\Delta_r = 1 - 2\epsilon_K$ is the gap between the optimal arm and any sub-optimal one. During the τ rounds during which the algorithm has not yet identified π^* .

We lower bound regret by considering only the rounds in which the algorithm plays $\hat{\pi}$ (an arm that incurs regret Δ_r since $\hat{\pi} \neq \pi^*$). To accumulate evidence distinguishing H_0 from H_1 , the algorithm must observe rewards from *both* arms. By an averaging argument on any τ -round policy: the number of times $\hat{\pi}$ is played satisfies $\mathbb{E}[\text{plays of } \hat{\pi}] \geq \mathbb{E}[\tau]$, since any algorithm that plays $\hat{\pi}$ fewer than τ times in expectation cannot attain type-I error $\leq \delta$ by the Wald bound (it lacks sufficient observations of H_0). Hence $\mathbb{E}[\text{regret}] \geq (1-\delta)\Delta_r\mathbb{E}[\tau] \geq (9)^*$. ■

F.2 Proof of Proposition 3

Proof (i) *Retention.* Let P, Q be the marginal joint distributions of $(\pi^*, \hat{\pi})$ for the training and testing distribution, respectively. By the chain rule: $D_{\text{KL}}(Q\|P) = \mathbb{E}_Q[D_{\text{KL}}(Q_{\hat{\pi}|\pi^*}\|P_{\hat{\pi}|\pi^*})] \leq \sup_{\pi^*} D_{\text{KL}}(Q_{\hat{\pi}|\pi^*}\|P_{\hat{\pi}|\pi^*}) = \Delta_\pi$. By Pinsker: $\|P - Q\|_1 \leq \sqrt{2\Delta_\pi}$. Since $I(X; Y) = H(X) + H(Y) - H(X, Y)$, by the triangle inequality

$$|I_P(\pi^*; \hat{\pi}) - I_Q(\pi^*; \hat{\pi}')| \leq |H_P(\hat{\pi}) - H_Q(\hat{\pi}')| + |H_P(\pi^*, \hat{\pi}) - H_Q(\pi^*, \hat{\pi}')|,$$

where the $|H(P_\pi^*) - H(Q_\pi^*)| = 0$ since $P_{\pi^*} = Q_{\pi^*} = \mu$. Applying entropy continuity (Csiszár-Körner) with $\varepsilon = \|P - Q\|_1 \leq \sqrt{2\Delta_\pi}$:

$$|I_P - I_Q| \leq 3\varepsilon \log K + 2h(\varepsilon/2) \leq 3\varepsilon \log K + \varepsilon \log(2/\varepsilon).$$

Set $\varepsilon = \sqrt{2\Delta_\pi} = R_{\text{mech}}^{\text{train}}/(K \log K)$. The combined bound now becomes

$$3\varepsilon \log K + \varepsilon \log(2/\varepsilon) = \frac{R_{\text{mech}}^{\text{train}}}{K \log K} \left(3 \log K + \log \frac{2K \log K}{R_{\text{mech}}^{\text{train}}} \right),$$

using $h(p) \leq -p \log p$ for $p \leq 1/e$ (satisfied since $\varepsilon/2 \leq 1/(2 \ln 12) \approx 0.042 < 1/e$ for $K \geq 12$). For this to be less than $R_{\text{mech}}^{\text{train}}/2$, setting $u = 2K \log K / R_{\text{mech}}^{\text{train}}$, the requirement becomes $\log u \leq (K/2 - 3) \log K$, i.e.

$$R_{\text{mech}}^{\text{train}} \geq 2K^{4-K/2} \log K := R_{\text{min}}(K).$$

Since

$$\frac{1}{K \log K} \left(3 \log K + \log \frac{2K \log K}{R_{\text{mech}}^{\text{train}}} \right)$$

decreases with $R_{\text{mech}}^{\text{train}}$, the worst-case is at $R_{\text{mech}}^{\text{train}} = R_{\text{min}}$. Thus, it suffices to verify the bound for $R_{\text{mech}}^{\text{train}} = R_{\text{min}}$.

For $K = 12$, $R_{\text{min}} = 2 \times 12^{-2} \times \ln 12 \approx 0.035$ nats. The bound then becomes $3 \times 0.035/12 + \frac{0.035}{12 \ln 12} \ln \frac{2 \times 12 \ln 12}{0.035} \approx 0.00875 + 0.00873 = 0.01748 < 0.0175 = R_{\text{min}}/2$. For all $K \geq 12$ the threshold $R_{\text{min}}(K)$ decreases rapidly, and the bound holds for any $R_{\text{mech}}^{\text{train}} \geq R_{\text{min}}(K)$. Hence $|I_P - I_Q| < R_{\text{mech}}^{\text{train}}/2$, giving $R_{\text{LLM}} \geq \frac{1}{2} R_{\text{mech}}^{\text{train}}$.

(ii) *Impossibility.* Construct the test distribution as follows: on half the indices $\pi^* \in \Pi$ assign the same conditional recommendation distribution as P_{train} (a fraction $\frac{1}{2}$ of the mixture); on the other half, reverse the recommendation so that $\hat{\pi} \mapsto \Pi \setminus \{\hat{\pi}\}$ uniformly. Formally, let $Q_{\hat{\pi}|\pi^*}(\cdot) = P_{\hat{\pi}|\pi^*}(\cdot)$ for $\pi^* \in S$ and $Q_{\hat{\pi}|\pi^*}(\cdot) = \text{Uniform}(\Pi)$ for $\pi^* \notin S$, where $|S| = K/2$. Keep the marginal $Q_\pi^* = P_\pi^* = \mu$. Then, since $Q_\pi^* = P_\pi^* = \mu$, the chain rule gives $D_{\text{KL}}(Q\|P) = \mathbb{E}_\mu[D_{\text{KL}}(Q_{\hat{\pi}|\pi^*}\|P_{\hat{\pi}|\pi^*})]$.

*This argument bounds regret from the plays of the suboptimal arm $\hat{\pi}$ only; the $(1-\epsilon)$ factor comes from the prior weight on $\hat{\pi}$ and is tight when the algorithm must spend time observing both hypotheses.

For $\pi^* \in S$: $D_{\text{KL}} = 0$; for $\pi^* \notin S$: $D_{\text{KL}}(\text{Uniform} \| P_{\hat{\pi}|\pi^*}) = \log K - H_P(\hat{\pi}|\pi^* = \cdot)$ (entropy of the point-conditional, not the average). Averaging over $\pi^* \notin S$ under uniform μ : $\mathbb{E}_{\pi^* \notin S}[D_{\text{KL}}] = \log K - H_P(\hat{\pi}|\pi^*)$ where $H_P(\hat{\pi}|\pi^*) = \mathbb{E}_{\pi^*}[H(P_{\hat{\pi}|\pi^*})]$ is the average conditional entropy. Hence $D_{\text{KL}}(Q \| P) = \frac{1}{2}(\log K - H_P(\hat{\pi}|\pi^*)) \leq \frac{1}{2} \log K$. Under Q , we bound I_Q using the *conditional entropy of the recommendation*: since for $\pi^* \in S$ the conditional $Q_{\hat{\pi}|\pi^*} = P_{\hat{\pi}|\pi^*}$ and for $\pi^* \notin S$ it equals $\text{Uniform}(\Pi)$:

$$H_Q(\hat{\pi} | \pi^*) = \frac{1}{2}H_P(\hat{\pi} | \pi^*) + \frac{1}{2} \log K.$$

Since $H_Q(\hat{\pi}) \leq \log K$:

$$\begin{aligned} I_Q(\pi^*; \hat{\pi}) &= H_Q(\hat{\pi}) - H_Q(\hat{\pi} | \pi^*) \\ &\leq \log K - \left(\frac{1}{2}H_P(\hat{\pi} | \pi^*) + \frac{1}{2} \log K\right) \\ &= \frac{1}{2}(\log K - H_P(\hat{\pi} | \pi^*)) \\ &\leq \frac{1}{2} \log K. \end{aligned}$$

The KL shift is $D_{\text{KL}}(Q \| P) = \frac{1}{2}(\log K - H_P(\hat{\pi} | \pi^*)) = \frac{1}{2}R_{\text{mech}}^{\text{train}} + \frac{1}{2}(\log K - H_P(\hat{\pi})) \leq \frac{1}{2} \log K$ (since $H_P(\hat{\pi}) \geq 0$). When $P_{\hat{\pi}}$ is uniform, $D_{\text{KL}}(Q \| P) = \frac{1}{2}R_{\text{mech}}^{\text{train}}$. In general $R_{\text{LLM}} \leq \frac{1}{2} \log K$. When $P_{\hat{\pi}}$ is uniform: $R_{\text{LLM}} \leq \frac{1}{2}(\log K - H_P(\hat{\pi}|\pi^*)) = \frac{1}{2}R_{\text{mech}}^{\text{train}}$ and $D_{\text{KL}}(Q \| P) = \frac{1}{2}R_{\text{mech}}^{\text{train}} \leq \frac{1}{2} \log K$. ■

As mentioned earlier, this proposition highly motivates the use of informed ODE priors over LLM priors. We now show this using our running example.

G Additional Experiment Details

Real-data motivation. In a prospective 37-site German cohort of 434 patients [27], only 20.3% of BSA-dosed patients reached the therapeutic target AUC range of 20–30 mg·h/L; 60.6% were underdosed and 19.1% overdosed. Saif et al. [35] summarize that across studies, only 20–30% of BSA-dosed patients achieve therapeutic exposure [35]. The consequences are large: the Gamelin et al. [14] randomized trial found PK-guided dosing achieved a 39% response rate versus 19% for BSA dosing ($p = .0004$), with median OS 22 vs. 16 months and significantly fewer toxic events ($p = 0.003$) [14]. A meta-analysis of four prospective trials ($N = 504$) confirmed 50–200% response rate improvement and $\approx 60\%$ reduction in grade 3/4 toxicity [12].

The learning problem. The key clinical bottleneck is the number of cycles required for the algorithm to converge to a patient’s optimal dose. Kaldate et al. [20] characterize the dose-AUC relationship in 187 FOLFOX6 patients (307 cycle-pair observations) as $\Delta\text{AUC} = 0.021 \times \Delta\text{dose mg/m}^2$ ($R^2 = 0.51$, $n = 307$) [20]. The moderate R^2 reflects the large individual variability in 5-FU clearance — up to 100-fold in C_{ss} across patients on the same BSA-based dose — driven by DPD genotype, sex, age, and hepatic function. The intra-patient cycle-to-cycle AUC variability is approximately 20%, motivating the 10 mg·h/L target window width [20].

Sex differential. Females clear 5-FU $\approx 21\%$ slower, producing mean AUC excess of 2.5 mg·h/L under standard BSA dosing [13]. However, between-sex variance accounts for only 3.6% of total log-AUC variance versus 86% from individual variation [13]. The 3.6% figure reflects the partial compensation between lower clearance and lower BSA in females; clinical toxicity studies [40] report disproportionately larger downstream effects on patient safety, driven by the asymmetric consequences of overdosing. The algorithm must individualize, not stratify by sex, since sex-specific clearance is handled by the ODE’s circadian-modulated clearance model, not by arm selection.

Burn-in. Proposition 2 gives a formal lower bound on the cost of a confidently-wrong prior. For the $K = 8$ calibrated setting with $\epsilon = 0.15$ and $\delta = 0.10$, the lower bound evaluates to ≈ 0.11 cycles, and the actual expected burn-in is roughly 1–2 cycles (see Running Example on burn-in). This is consistent with Capitain et al. [5]: 94% of 118 PK-adjusted FOLFOX patients achieved the target AUC within two monitored cycles.

Prior construction. The policy described by Theorem 2, the policy that is recommended by the mechanistic model ($\hat{\pi}$) satisfies $I(\hat{\pi}; \pi^*) = R_{\text{mech}}$. To create such a policy we selected the policy such that $\hat{\pi}$ for the recommended decision will be β and for all other policies, α where $\alpha \leq \beta$ and $\beta + (K - 1)\alpha = 1$, $H(\hat{\pi}) = 1$. This policy was found using a black-box optimizer.

Compute. The experiments were done on the author’s personal machine using CPU only and do not require any special computing.

H Calibration of the 5-FU example

The running examples evaluate the channel bound (3) and the critical-bias threshold (8) at the working values

$$K = 8, \quad \sigma = 0.40, \quad \kappa_\mu = 1.8, \quad d_F = 3, \quad B_\mu = 0.22, \quad H(\mu) = \ln K = 2.0794 \text{ nats.}$$

This appendix specifies the provenance of each value. We distinguish three categories. *Identifiable from primary sources:* σ , $H(\mu)$, the dose–AUC slope S , the target window, the infusion horizon T , and the BSA-baseline target attainment p_{BSA} . *Determined by a stated normalisation convention:* κ_{ss} (the steady-state component of κ_μ) and p_{opt} (a single-point summary of the multi-source PK-guided literature). *Rationalized from public 5-FU literature:* K , κ_μ , d_F , and B_μ . Each value is anchored qualitatively in the published 5-FU literature without being directly measurable from public datasets at the precision required by Eqs. (3) and (8); we therefore state the working value, justify it from named clinical sources, and verify via the sensitivity analysis of Section H.5 that the qualitative classification of Running Example 4 holds across the plausible range of each parameter.

The composite certificate at the working values is computed in Section H.4, and the sensitivity of the certificate to each parameter is reported in Section H.5.

H.1 Quantities identifiable from primary sources

Dose–AUC slope $S = 0.02063 \text{ (mg} \cdot \text{h/L)}/(\text{mg/m}^2)$. Linear regression of ΔAUC on Δdose across $n = 307$ cycle-pair observations from 187 FOLFOX6 patients in the Kaldate et al. [19] database, with $R^2 = 0.51$ and dose range $[1,600, 3,600] \text{ mg/m}^2$. We use S in equation (2) below.

Therapeutic window $[20, 30] \text{ mg} \cdot \text{h/L}$ and **infusion horizon** $T = 46 \text{ h}$. Standard FOLFOX6 conventions; consistent in Kaldate [20], Capitain [5], Saif [35], Wilhelm [42], and Fleming [13].

BSA-baseline target attainment $p_{\text{BSA}} = 0.203$. Li et al. [26], $n = 434$ prospective multicentre cohort: “Only 20.3% of all patients reached the target range of 5-FU AUC.” We use $p_{\text{BSA}} = 0.20$ in subsequent arithmetic.

Reward-observation noise $\sigma = 0.40$. The reward $r_t = \mathbf{1}\{\text{AUC}_t \in [20, 30]\} \in \{0, 1\}$ is Bernoulli, so the noise of Section 2.1 is $\sigma_r(\bar{r}) = \sqrt{\bar{r}(1 - \bar{r})}$. At $\bar{r} = p_{\text{BSA}} = 0.20$,

$$\sigma = \sqrt{0.20 \cdot 0.80} = 0.40. \quad (14)$$

The single- σ homoscedastic approximation in Proposition 1 incurs an absolute error bounded by $\max_{\bar{r} \in [0,1]} \sqrt{\bar{r}(1 - \bar{r})} - \sigma = 0.10$; the sensitivity sweep over $\sigma \in [0.357, 0.50]$ in Section H.5 brackets this error.

Prior entropy $H(\mu) = \ln K$. Definitional: the prior μ on Π is the maximum-entropy choice in the absence of patient-specific information. $K = 8$ is itself a discretisation choice, treated in Section H.3.

H.2 Quantities determined by a stated normalisation convention

Steady-state policy sensitivity κ_{ss} . Let u_{raw} denote dose in mg/m^2 and y_{raw} AUC in $\text{mg} \cdot \text{h/L}$. Fix dimensionless coordinates by $u_{\text{norm}} = u_{\text{raw}}/U$ and $y_{\text{norm}} = y_{\text{raw}}/Y$ with normalisation constants $U = 2,000 \text{ mg/m}^2$ (the Kaldate dose-range width $3,600 - 1,600$) and $Y = 25 \text{ mg} \cdot \text{h/L}$ (target window centre). By the chain rule, $\partial u_{\text{norm}}/\partial y_{\text{norm}} = (Y/U) \cdot (\partial u_{\text{raw}}/\partial y_{\text{raw}}) = (Y/U) \cdot (1/S)$. Substituting,

$$\kappa_{\text{ss}} = \frac{Y}{U \cdot S} = \frac{25}{2,000 \times 0.02063} = 0.606. \quad (15)$$

κ_{ss} is the steady-state component of κ_μ : it captures the static dose-to-AUC sensitivity but not the cumulative dynamics of the 46-hour infusion or the curvature of the value functional, both of which enter the full κ_μ via the linearised state–costate system (Lemma 1).

PK-guided target attainment $p_{opt} = 0.85$. Reported values for FOLFOX-class regimens vary with regimen, dose-adjustment algorithm, cycle index, and definition:

Source	Cohort and protocol	Reported attainment
[29]	$n = 75$ FOLFOX/AIO/FUFOX, PK-adjusted from cycle 2	0.49, 0.67, 0.61 at cycles 1, 2, 3
[5]	$n = 118$ FOLFOX, PK-adjusted (ODPM)	0.70 ORR (different endpoint)
[14]	$n = 208$ weekly LV5FU2 (not FOLFOX), PK-adjusted	0.94 successful adjustment

We summarise the literature by a single working value $p_{opt} = 0.85$, an interior point of the reported range. Section H.5 reports the sensitivity over $p_{opt} \in [0.50, 0.95]$.

H.3 Quantities rationalized from public 5-FU literature

The four parameters K , d_F , κ_μ , and B_μ are not directly extractable from published 5-FU datasets at the precision required by Eqs. (3) and (8). For each we state the working value, give a literature-grounded rationale, and verify in Section H.5 that the qualitative classification holds across the plausible sweep range.

Number of arms $K = 8$. A discretisation choice. The Kaldate adjustment range [1,600, 3,600] mg/m² is partitioned into 8 equal levels with grid spacing 250 mg/m², comparable to the smallest dose adjustments reported in Kaldate’s protocol (145 mg/m²). We sweep $K \in \{4, 6, 8, 10, 12, 16\}$.

Effective residual dimension $d_F = 3$. Under Assumption 3, d_F is a measure of the effective rank of the kernel operator \mathcal{K}_μ of the residual GP g^* . With eigenvalues $\lambda_1 \geq \lambda_2 \geq \dots \geq 0$ of \mathcal{K}_μ , the operationalisation we adopt is the participation ratio

$$d_F = \frac{(\sum_i \lambda_i)^2}{\sum_i \lambda_i^2} = \frac{\text{tr}(\mathcal{K}_\mu)^2}{\text{tr}(\mathcal{K}_\mu^2)}. \quad (16)$$

Empirical estimation of d_F requires fitting g^* on a held-out cohort with per-patient AUC measurements and the relevant covariates; no public 5-FU dataset combines both at the scale required. We use $d_F = 3$ as a working value, consistent with the count of near-orthogonal covariate clusters that drive between-patient 5-FU clearance variability after BSA adjustment:

- (i) DPYD genotype or U/UH₂ phenotype, the dominant categorical effect on hepatic DPD-mediated clearance (Saif [32]).
- (ii) Hepatic function (bilirubin, albumin, alkaline phosphatase) modulating clearance independently of DPYD (Saif [32]).
- (iii) Body composition beyond BSA, captured by sex and skeletal muscle index (Wagner et al. [37], ACCENT $n = 34,640$).

The cluster count is an upper bound on d_F in (3) since the modes are not strictly orthogonal. We sweep $d_F \in \{2, 3, 4, 5\}$. Note that d_F is not the dimension of the ODE state space (here 5). The ODE compartments are deterministic transformations of dose, clearance, and time once the patient parameters are fixed; only the residual variability that persists after the model has been applied contributes to d_F .

Occupancy-weighted Lipschitz constant $\kappa_\mu = 1.8$. By Lemma 1 (Appendix C.1), κ_μ is the $L^2([0, T])$ operator norm of the linearised state–costate system along the unperturbed optimal trajectory. Numerical evaluation of this norm requires integrating the Riccati equation along the Fleming [12] ODE under patient-specific clearance and circadian modulation; this is outside the scope of the present work. We use $\kappa_\mu = 1.8 \approx 3\kappa_{ss}$. The factor of three collapses two distinct effects — the cumulative response of the integrated reward to the 46-hour infusion, and the Hamiltonian

curvature near the optimum — into a single multiplier. We sweep $\kappa_\mu \in [0.6, 3.0]$, the lower endpoint corresponding to $\kappa_\mu = \kappa_{ss}$ (no dynamic correction) and the upper endpoint to a substantial overestimate.

Model bias $B_\mu = 0.22$. By Assumption 2, $B_\mu = \|J(\cdot; \mathcal{M}) - J(\cdot; \hat{\mathcal{M}})\|_{\mu, \pi^*}$. For the Bernoulli reward of Section 5.1 the value functional reduces to the per-arm in-target probability $J(\pi) = \Pr\{\text{AUC} \in [20, 30] \mid \pi\}$, so

$$B_\mu^2 = \sum_{k=1}^K w_k (p_{\pi_k}^{\text{true}} - p_{\pi_k}^{\text{model}})^2, \quad (17)$$

the occupancy-weighted RMS deviation between the population in-target fraction at each arm and the Fleming [12] ODE prediction at that arm. B_μ measures model error, not patient-level variability.

The public 5-FU literature constrains exactly one of the eight arms in Π . Li [26] reports $p_{\text{BSA}}^{\text{true}} = 0.203$ for BSA-dosed patients, which fixes the contribution of the BSA arm to (4) once $p_{\text{BSA}}^{\text{model}}$ is computed from the calibrated ODE. The remaining seven arms have no comparable public anchor: no published cohort reports per-cycle in-target proportions stratified by dose level across the full [1,600, 3,600] mg/m² range. Direct estimation of B_μ from public data is therefore not feasible. We use $B_\mu = 0.22$ as a working value, sweep $B_\mu \in [0.10, 0.40]$, and report in Section H.5 that the qualitative classification holds across this range.

In particular: bounds derived from the Kaldate $R^2 = 0.51$ characterise the inter-patient variability of ΔAUC given Δdose , not the gap between $p_{\pi_k}^{\text{true}}$ and $p_{\pi_k}^{\text{model}}$ that defines B_μ in (4). A perfectly calibrated mechanistic model can produce $B_\mu = 0$ while leaving Kaldate’s R^2 unchanged at 0.51, and conversely. Calibration of B_μ against the Kaldate R^2 would therefore conflate distinct sources of variation.

H.4 Composite certificate at the working values

Substituting $\sigma = 0.40$, $\kappa_\mu = 1.8$, $d_F = 3$, $H(\mu) = \ln 8$, $B_\mu = 0.22$, $N = 12$ into the canonical parametrization of Remark 2 and into bounds (3) and (8):

$$\sigma_F^2 = \frac{2\sigma^2 H(\mu)}{\kappa_\mu^2 d_F} = \frac{2(0.16)(2.0794)}{(3.24)(3)} = 0.0685, \quad (18)$$

$$C(B_\mu) = \frac{d_F}{2} \ln \left(1 + \frac{\kappa_\mu^2 \sigma_F^2}{\kappa_\mu^2 B_\mu^2 + \sigma^2} \right) = 1.5 \ln(1.700) = 0.796 \text{ nats}, \quad (19)$$

$$H_{\text{mech}} \geq H(\mu) - C(B_\mu) = 1.283 \text{ nats}, \quad (20)$$

$$B_\mu^{\text{crit}}(N) = \frac{\sigma}{\kappa_\mu} \sqrt{\frac{2H(\mu)/d_F}{\exp(2H(\mu)/(d_F N)) - 1}} - 1. \quad (21)$$

At $N = 12$, the last equation evaluates to $B_\mu^{\text{crit}}(12) = 0.714$. The classification $B_\mu = 0.22 < B_\mu^{\text{crit}}(12) = 0.714$ holds with margin $B_\mu^{\text{crit}}/B_\mu = 3.24$.

H.5 Sensitivity analysis

Each calibration parameter is varied over its sweep range with the remaining parameters held at the working values. Table 4 reports the resulting ranges for $C(B_\mu)$ and $B_\mu^{\text{crit}}(N)$ at $B_\mu = 0.22$ and $N = 12$. The qualitative classification is most sensitive to κ_μ , which sets the policy-to-value scale. At the lower endpoint $\kappa_\mu = \kappa_{ss} = 0.6$, the channel is highly informative with $C(0.22) = 1.22$ nats and $B_\mu^{\text{crit}}(12) = 2.14$. At the upper endpoint $\kappa_\mu = 3.0$, the certificate tightens to $C(0.22) = 0.47$ nats and $B_\mu^{\text{crit}}(12) = 0.43$, still above $B_\mu = 0.22$ by a factor of 1.95. The classification $B_\mu < B_\mu^{\text{crit}}$ therefore holds across the entire range of κ_μ we entertain.

The same sensitivity surface is depicted in Figure 2. The top row plots channel capacity $C(B_\mu)$ as a 1D function of each parameter individually, holding the other two at their calibrated values; the bottom row plots the certificate ratio $B_\mu/B_\mu^{\text{crit}}$ as 2D heatmaps over each parameter pair, with the white contour at ratio = 1 marking the phase boundary between the data-efficient regime (blue, prior

Parameter	Sweep range	C_{\min}	C_{\max}	B_{\min}^{crit}	B_{\max}^{crit}
σ (via σ_r at $\bar{r} \in \{p_{\text{BSA}}, 1/2\}$)	[0.357, 0.50]	0.73	0.92	0.64	0.89
κ_{μ}	[0.6, 3.0]	0.47	1.22	0.43	2.14
$d_{\mathcal{F}}$	{2, 3, 4, 5}	0.72	0.88	0.70	0.72
K (via $H(\mu) = \ln K$)	{4, 6, 8, 10, 12, 16}	0.57	0.99	0.71	0.72
p_{opt} (via $\sigma = \sqrt{p_{\text{opt}}(1 - p_{\text{opt}})}$)	[0.50, 0.95]	0.42	0.92	0.39	0.89
B_{μ}	[0.10, 0.40]	0.42	1.15	0.71	0.71

Table 4: Sensitivity of $C(B_{\mu} = 0.22)$ and $B_{\mu}^{\text{crit}}(N = 12)$ to each parameter. The classification $B_{\mu} < B_{\mu}^{\text{crit}}$ holds in every cell. B_{μ}^{crit} is independent of B_{μ} , hence the constant value in the last row.

helps) and the baseline regime (red, prior is too biased to be useful). The calibrated 5-FU operating point sits comfortably inside the data-efficient region in every panel.

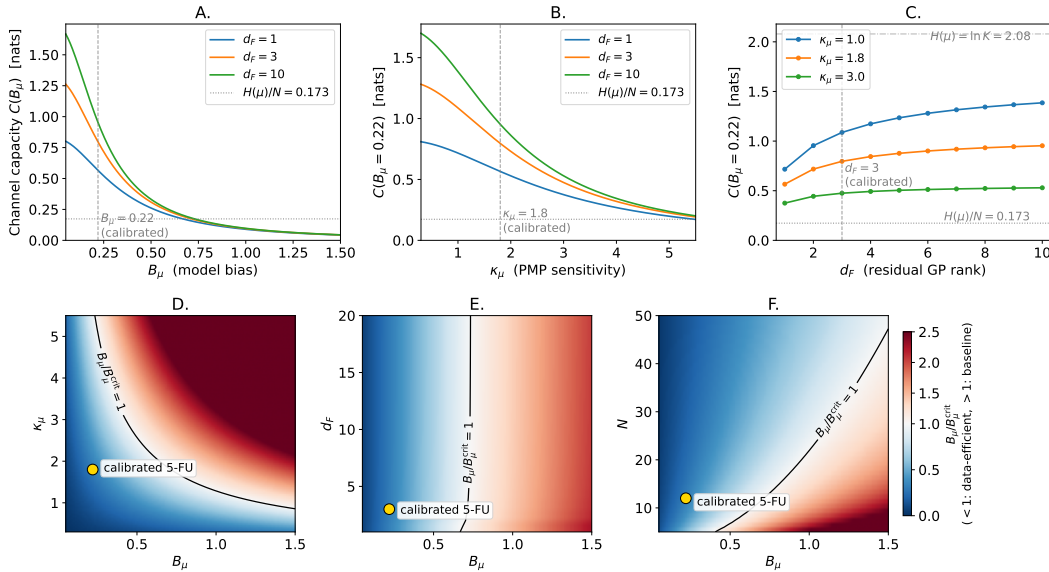


Figure 2: Sensitivity of the model-quality certificate to parameters κ_{μ} (PMP sensitivity), B_{μ} (model bias), and $d_{\mathcal{F}}$ (residual GP rank). Top row: Channel capacity $C(B_{\mu})$ as a function of each parameter, with the calibrated 5-FU operating point indicated by vertical dashed lines. Bottom row: Heatmaps of the ratio $B_{\mu} / B_{\mu}^{\text{crit}}$ over parameter pairs, colored by the ratio value (red for >1 , blue for <1), with the phase boundary ($B_{\mu} / B_{\mu}^{\text{crit}} = 1$) marked by black contours. The calibrated point is denoted by a gold dot (\bullet). Values below 1 indicate data-efficient regimes.

Figure 2 sweeps κ_{μ} , B_{μ} , and $d_{\mathcal{F}}$ at fixed $K = 8$. Figure 3 extends the sensitivity treatment to the discretization choice K , the only working parameter not varied in Figure 2 plots the phase-transition threshold $B_{\mu}^{\text{crit}}(N = 12)$ against K ; the threshold is essentially flat across $K \in [2, 20]$ (it varies only through $H(\mu) = \ln K$ inside (8), a logarithmic dependence), and the calibrated $B_{\mu} = 0.22$ sits well within the shaded data-efficient region across the entire range.

As illustrated in Figures 2 and 3, the values of the calibrated variables introduce only marginal changes to B_{μ} . This insensitivity further validates the primary conclusions of the analysis presented in Section 5.

H.6 Summary of working values and provenance

Table 5 consolidates the working values and their provenance.

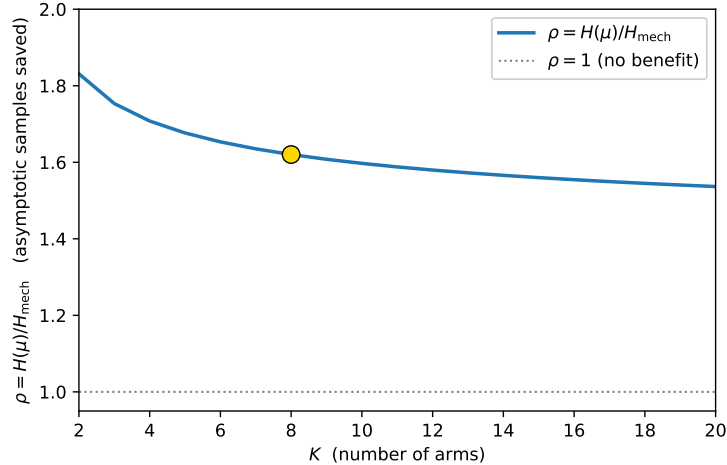


Figure 3: Critical bias as a function of K . The blue curve corresponds to the theoretical sample complexity ratio. The dotted line corresponds with the baseline ratio ($\rho = 1$). All other parameters held at their calibrated values ($B_\mu = 0.22$, $\sigma = 0.40$, $\kappa_\mu = 1.8$, $d_F = 3$, $N = 12$).

Parameter	Working value	Provenance	Sweep range
T	46 h	FOLFOX6 standard [13, 20]	—
Target window	[20, 30] mg · h/L	Standard [5, 20, 35]	—
S	0.02063	Kaldate [20], $n = 307$, $R^2 = 0.51$	—
p_{BSA}	0.203	Li [27], $n = 434$	—
σ	0.40	$\sqrt{p_{\text{BSA}}(1 - p_{\text{BSA}})}$	[0.357, 0.50]
$H(\mu)$	$\ln 8$	Definitional, K uniform	—
κ_{ss}	0.606	Equation (2); normalisation U , Y	—
p_{opt}	0.85	Mid-range across [5, 14, 42]	[0.50, 0.95]
K	8	Discretisation; gap 250 mg/m ²	{4, ..., 16}
κ_μ	1.8	$\approx 3\kappa_{\text{ss}}$; not numerically derived	[0.6, 3.0]
d_F	3	Three covariate clusters; eq. (3)	{2, 3, 4, 5}
B_μ	0.22	Working value; illustrated using public data	[0.10, 0.40]

Table 5: Provenance and sweep range for each parameter. The data-efficient classification $B_\mu < B_\mu^{\text{crit}}$ holds across all sweeps in Table 4.

H.7 Scope and outlook

The contribution of this work is computational and theoretical: the bounds, the certificate, and the calibration tiers establish the conditions under which a hybrid mechanistic-plus-stochastic prior provides quantifiable benefit over the uninformed baseline, and they identify the parameters whose values control that benefit. The 5-FU instantiation demonstrates that these conditions can be partially anchored in published clinical literature — the noise scale σ , the dose–AUC slope S , and the BSA–baseline target attainment p_{BSA} are derived from primary sources — and identifies, through the tier classification, which parameters require additional measurement.

Translating the framework into actionable claims about the value of a specific mechanistic model for a specific clinical task requires three steps that are outside the scope of a methodological paper. First, a fully specified ODE (here the 5-compartment Fleming [12] model) must be calibrated to a population mean and integrated to produce per-arm predictions $p_{\pi_k}^{\text{model}}$. Second, a held-out validation cohort with per-patient AUC measurements distributed across the policy class is needed to anchor B_μ via (4), the Riccati integration of Lemma 1 along the calibrated trajectory is needed to anchor κ_μ , and per-patient covariates spanning the three clusters of Section H.3 are needed to anchor d_F via (3). Third, with

these calibrations in place, the certificate $C(B_\mu)$ becomes a quantitative statement about a particular mechanistic model on a particular drug — and the gap between the certificate and the empirical regret on the validation cohort becomes a measurement of the residual mechanistic information not captured by the bounds. Pursuing this program for 5-FU would convert the framework from a theoretical construction into a tool for evaluating which components of the Fleming model (for example) contribute most to the prior's value and which biological covariates merit measurement at the bedside; carrying out this program for 5-FU, and developing analogous programs for other drugs, are natural directions for follow-on clinical work.